EUROPEAN JOURNAL OF PHYCOLOGY
2024, VOL. 59, NO. 3, 311–331
https://doi.org/10.1080/09670262.2024.2343088

Pseudanabaena pruinosa sp. nov. (Pseudanabaenales, Cyanobacteria): an Arctic *Pseudanabaena* species with branched sheaths and central aerotopes

Boris Aleksovski[a], Svetislav Krstić[a], Jiří Komárek[b], Kim Nguyen[c], Kiril Pakovski[a], Sanja Kiprijanovska[d], Aleksandar Dimovski[d], Ana Vuchurević[a], Evgenija Stefanoska[a] and Otakar Strunecký[c]

[a]Faculty of Natural Sciences and Mathematics-Skopje, Institute of Biology, Ss. Cyril and Methodius University in Skopje, Arhimedova 3, PO Box 162, Skopje 1000, North Macedonia; [b]Czech Academy of Sciences, Institute of Botany, Dukelská 135, Třeboň CZ379 82, Czech Republic; [c]Faculty of Fisheries and Protection of Waters, CENAKVA, Institute of Aquaculture and Protection of Waters, University of South Bohemia in České Budějovice, Na Sádkách 1780, České Budějovice 370 05, Czech Republic; [d]Macedonian Academy of Sciences and Arts Skopje, Research Centre for Genetic Engineering and Biotechnology 'Georgi D Efremov', Skopje 1000, North Macedonia

ABSTRACT

This study focused on polyphasic evaluation of four psychrophilic *Pseudanabaena* strains collected from extreme environments characterized by freezing temperatures. The strains were isolated from hydroterrestrial and terrestrial ecosystems in Petuniabukta Bay (Billefjorden, Svalbard), growing as icy microbial soil crusts. In addition to their unique ecology, the phylogenetic analyses of 16S rRNA revealed that the strains form a monophyletic clade within the *Pseudanabaena sensu stricto* cluster; this clade was unambiguously separated from the other *Pseudanabaena* infrageneric units, showing <98.5% 16S rRNA sequence identity with the other *Pseudanabaena* strains available in GenBank and possessing a unique and different D1 ITS region. Polyphasic evaluation of these four strains led to the description of the new species *Pseudanabaena pruinosa* sp. nov. which can be morphologically distinguished by light microscopy by several unique apomorphic traits not previously detected in *Pseudanabaena*. These traits include: production of widened, anastomotic branched sheaths enveloping several trichomes into a filament, heteropolar filaments with long trichomes with more than 20 cells, richly pseudobranched filaments forming tree-like structures, production of both polar and central aerotopes, and ability to produce swollen cells and to undergo irregular cell division. The characters observed for *Pseudanabaena pruinosa*, never reported for other species of *Pseudanabaena*, substantially widen the taxonomic concept of this genus. Therefore, the description of *Pseudanabaena pruinosa* sp. nov. with its unique ecology and distinct phylogenetic position and morphological features, is a significant addition to cyanobacteriology and represents a starting point for further research into the evolution of the genus *Pseudanabaena*. The new combination *Pseudanabaena gygaxiana* (Casamatta & Johansen) Aleksovski, Krstić & Strunecký is proposed based on16S rRNA, supported by its shared phenotypic traits and similar ecology to *Pseudanabaena pruinosa*.

ARTICLE HISTORY Received 3 October 2023; Revised 1 March 2024; Accepted 6 April 2024

KEYWORDS *Arthronema gygaxiana*; branched sheaths; central aerotopes; *Pseudanabaena*; psychrotrophic species; Svalbard

Introduction

Although many cyanobacteria can survive in diverse environments, from polar to temperate and tropical regions, and from oceans to deserts, inhabiting terrestrial, freshwater and marine ecosystems (Komárek *et al.*, 2014), only a few species in a few particular genera are capable of thriving in all of them. *Pseudanabaena* Lauterborn and *Leptolyngbya* Anagnostidis & Komárek belong to these genera renowned for their versatility and 'special' ability to flourish in almost any ecosystem (Komárek & Anagnostidis, 2005).

The family Pseudanabaenaceae was first identified as a distinct taxonomic unit by Anagnostidis & Komárek (1988) using a morphology based approach. However, over time, the family descriptor of thin, more or less constricted cells in filaments led to continuous taxonomic change. In 2005, Komárek & Anagnostidis (2005) described 17 genera, and this later grew to 48, resulting in the formation of the order Pseudanabaenales (Komárek *et al.*, 2014). Recently, advances in molecular biology, particularly genomic sequencing, have divided the Pseudanabaenales into two families: Pseudanabaenaceae (Anagnostidis & Komárek, 1988) and Thalassoporaceae Strunecký & Mareš 2023 (Strunecký *et al.*, 2023). Despite these two families being morphologically identical, the newly formed family Thalassoporaceae was limited to marine and brackish species, while the Pseudanabaenaceae retained the planktic genus *Limnothrix* Mefert and the ecologically important genus *Pseudanabaena*. The remaining Pseudanabaenales genera were mostly moved to newly formed phylogenetically distant orders and families (Strunecký *et al.*, 2023).

The biological diversity of the genus *Pseudanabaena* is undeniably underestimated both genetically and

CONTACT Otakar Strunecký otakar.strunecky@gmail.com

Published online 16 Jul 2024

morphologically, but the strains with known 16S rRNA gene sequences and morphology are relatively consistent with the latest *Pseudanabaena* definition (Strunecký *et al.*, 2023). *Pseudanabaena* are homocytic unbranched filamentous cyanobacteria, with parietal thylakoids (Mareš *et al.*, 2019), sharing a very simple morphology of barrel-shaped, ~2 µm wide, ~3 µm long constricted cells, connected by structures later called 'hyaline bridges' (Skuja, 1948; Anagnostidis, 1961), corresponding with the iconotype, i.e. Lauterborn's illustration of *Pseudanabaena catenata* (Lauterborn, 1915, pl. III: fig. 27).

Despite the morphological simplicity of *Pseudanabaena* and its connection to the basal filamentous cyanobacterial lineages, this genus still deserves attention due to its ubiquitous nature and the broad, typically freshwater and soil, cosmopolitan distribution, consisting of sapropelic, epipelic or ednopelic, epiphytic, periphytic or metaphytic, secondary planktic and endogleic species (Komárek & Anagnostidis, 2005). Recently, *Pseudanabaena* has also been found to be well adapted to extreme environments, particularly in polar regions, where it inhabits challenging niches, and is diversified into distinct morphotypes and ecotypes under the pressure of frequently fluctuating and freezing temperatures, being able to survive freeze-thaw cycles (Pessi *et al.*, 2019). The wide occurrence of planktic and benthic *Pseudanabaena* species at Svalbard has been recently documented by light microscopy by Matula *et al.* (2007) and Davydov (2018). Matula *et al.* (2007) reported the presence of *P. catenata, P. galeata* Böcher, *P. limnetica* (Lemmermann) Komárek and *P. biceps* Böcher in Hornsund *et al.*, (2018) pointed out the frequent presence of *P. minima* (G.S.An) Anagnostidis in pools, in fast and slow streams, on seepages, and in sea marshes in Svalbard. Recent studies also revealed well-developed populations of *Pseudanabaena* in Antarctica (Averina *et al.*, 2020; Lumian *et al.*, 2024). Up to now, strains isolated from Svalbard and maintained in culture include: *P. catenata* USMAC16 from a small water body in Revdalen (Khan *et al.*, 2017), *Pseudanabaena* sp. LW0831 isolated from a snow-broth lake in Ny-Ålesund (Su *et al.*, 2017), and *Pseudanabaena* sp. CCALA 873 and *Pseudanabaena* sp. SPIC_04_40, isolated from soft brown biofilms in a shallow lake on a sea terrace in Hornsund (Aleksovski, 2015).

Field studies suggest large populations of *Pseudanabaena* spp. in Petuniabukta Bay, the northwestern branch of Billefjorden in the central part of Spitsbergen, Svalbard. Different morphotypes of *Pseudanabaena* were found in fast glacial streams, tundra pools, seepages on slopes and coastal brackish puddles (Komárek *et al.*, 2012). More recently, Pessi *et al.* (2019) reported the presence of Pseudanabaenales in the deglaciated, proglacial biological soil crusts in three glacier forefields (Ebba, Hørbyebreen and Ragnarbreen) on Petuniabukta Bay.

To assess the diversity of *Pseudanabaena* morphotypes, the area of Petuniabukta was sampled, and four strains from freshwater ecosystems and soil crusts were successfully isolated and maintained in culture. These strains constituted a morphologically and phylogenetically distinct group, which was clearly separated from the currently described species of *Pseudanabaena*. The polyphasic evaluation of these four strains led to the description of the new species *Pseudanabaena pruinosa* Aleksovski, Krstić, Komárek & Strunecký, which is detailed here. We also propose the new combination *Pseudanabaena gygaxiana* (Casamatta & Johansen) Aleksovski, Krstić & Strunecký based on phylogenetic analysis of 16S rRNA, supported by its phenotypic and ecological proximity to *Pseudanabaena pruinosa*.

Materials and methods

Study area, field sampling and strain isolation

The study area and the sampling sites were located around Petuniabukta Bay, Billefjorden, Svalbard (Fig. 1). During 2011, icy microbial soil crusts were sampled from hydro-terrestrial ecosystems (two samples collected from the foreland of the valley glacier Hørbyebreen, i.e. from the ice front of its marginal zones, contained the strains NMCCC 001 and NMCCC 013) and a terrestrial ecosystem (sample from Mumien Peak summit, 773 m above sea level, included the strain NMCCC 014). In August 2015, strain NMCCC 002 was isolated from a hydro-terrestrial ecosystem, with *Hydrurus foetidus* as the dominant species in this fast-flowing glacial stream fed from melting glaciers on Fortet Mountain (detailed field images are provided in Komárek *et al.*, 2012) (Fig. 4). More details concerning the ecology of the four strains are given in Table 1.

The mats collected from Petuniabukta were sent to the Centre of Algology at the Institute of Botany (Czech Academy of Sciences, Třeboň). Unialgal strains were isolated and shipped to the Laboratory for Hydrobiology and Algal Culture in Skopje, North Macedonia, where they were included in the North Macedonia Culture Collection of Cyanobacteria (NMCCC).

At NMCCC all unialgal strains were grown both in liquid Z8 medium and on plates in solidified ½ Z8 medium with 0.7% agarose. The strains were placed on a bespoke system of shelves irradiated by horizontal panels of fluorescent cool white light at a photon irradiance of 43–81 µmol $m^{-2}s^{-1}$. The conditions were strictly controlled, with a 16:8 h light: dark

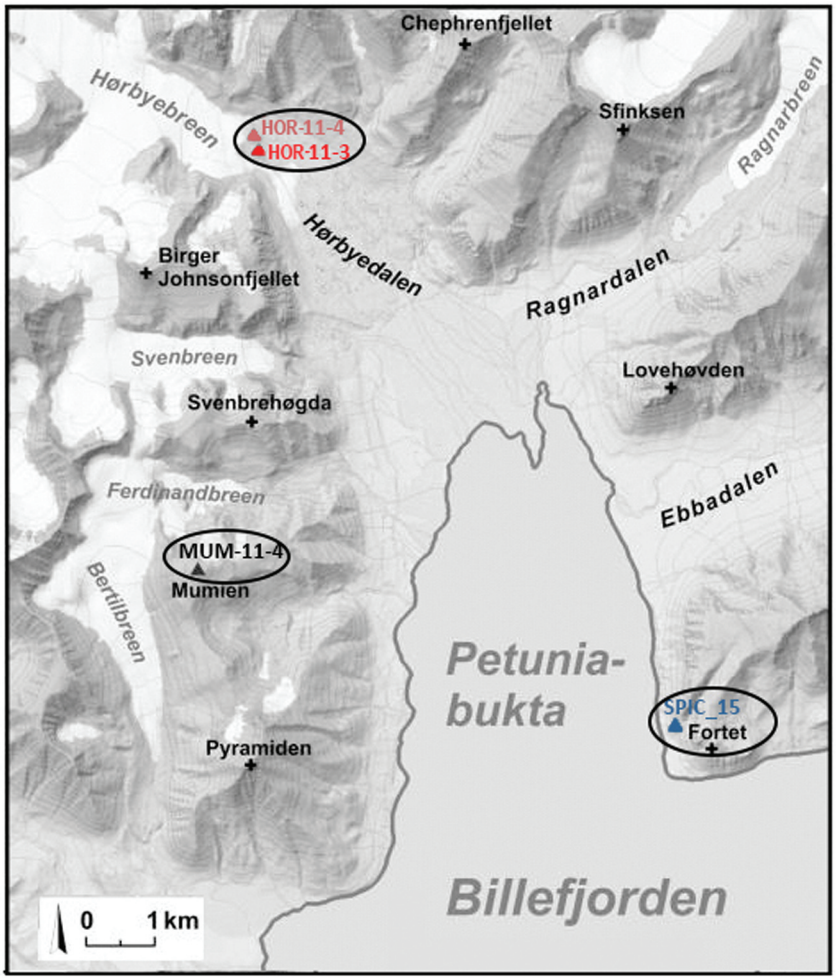

Fig. 1. Map of Petuniabukta Bay showing the location of the sampling sites. (Modified from Svalbardkartet data, Norwegian Polar Institute.).

cycle and a temperature range of 15–16°C. The strains were also grown in a closed phytotron at 6°C, under the same light conditions.

Strain growth rates

Specific growth rate (μ) of the strains was estimated using test tubes with 10 ml liquid Z8 medium. The tubes were inoculated with 100 µl of cell suspension and incubated at different temperatures (4°C, 8°C, 15°C, 22°C, 25°C; five replicates for each temperature) in the phytotron under controlled light conditions (photon irradiance of 47 µmol m^{-2} s^{-1}, supplied by cool white light fluorescent tubes, at 16:8 light: dark cycles). Absorbance was measured at 650 nm using a spectrophotometer after 7 days (A_7) and compared with the initial absorbance after inoculation (A_0). The specific growth rate was calculated using the formula:

$$\mu = (\ln A_7 - \ln A_0)/7$$

The initial absorbance of the cultures was similar for all temperature conditions (0.1084 ± 0.0085). Before reading the absorbance, the cultures were gently homogenized by pushing them through a 23-gauge syringe, followed by shaking.

Morphological analyses

Morphological assessments were made by light microscopy (LM) and epifluorescence microscopy, using a Nikon Eclipse E800M microscope equipped with a Nikon Coolpix 4500 digital camera, and Nikon Eclipse *Ni* equipped with a Canon EOS 600D camera. The following morphological characters were analysed: cell shape, trichome width (W), cell length (L), L:W ratio, presence of sheaths, motility, presence of aerotopes, presence and type of 'hyaline bridges', type of constrictions and presence of granules. For the determination of the cell length-to-width ratio (L:W), at least 100 cells were measured for each strain. To assess phenotypic plasticity, the strains were grown at different temperatures (4°C, 8°C, 15°C, 22°C, 25°C) and under three different irradiances (low – 44 µmol $m^{-2}s^{-1}$; medium – 65 µmol m^{-2} s^{-1}; and high – 83 µmol $m^{-2}s^{-1}$), and the differences in morphology were recorded.

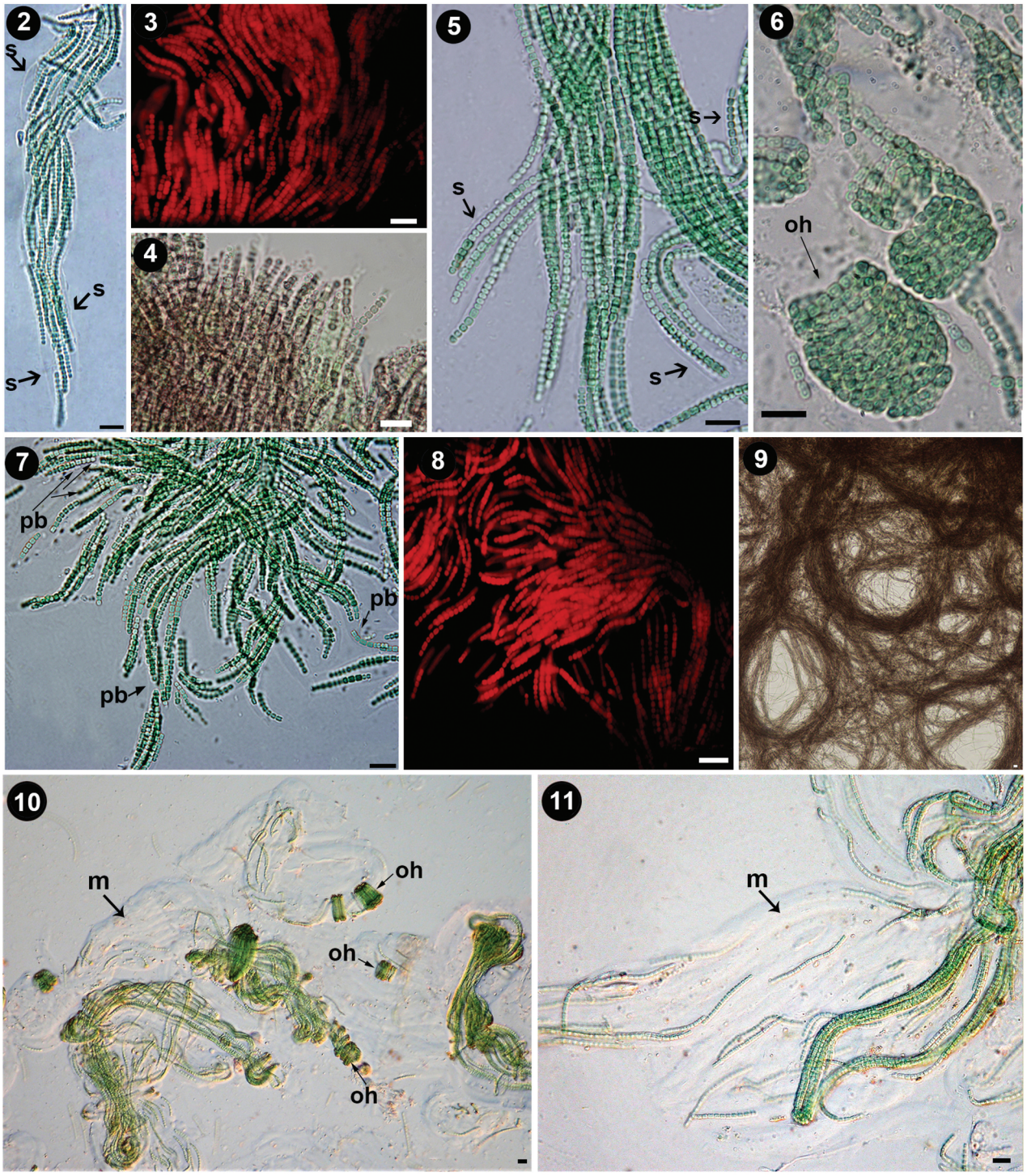

Figs 2–11. Morphological characters of *Pseudanabaena pruinosa* sp. nov. **Fig. 2**. Heteropolar, curved, and flexible filament of *P. pruinosa* NMCCC 001with a widened sheath, and clear refractive margins can be observed, containing several parallel entangled and fasciculate trichomes at the base, and a few solitary trichomes in the apical part of the single sheath. **Fig. 3**. UV epifluorescence micrograph of *P. pruinosa* NMCCC 001; trichomes closely grouped in parallel 'erected' positions can be observed. **Fig. 4**. Regular organization in erected fascicles in *P. pruinosa* NMCCC 002. **Fig. 5**. Divaricated, pseudobranched filaments, due to the presence of anastomotic branched sheaths in *P. pruinosa* NMCCC 001. A characteristic tree-like spreading of the filaments within the thallus can be observed. **Fig. 6**. Regular screw-like coils (left-handed open helixes) in mats of *P. pruinosa* NMCCC 013. **Fig. 7**. Clearly pseudobranched filaments, with tree-like spreading in *P. pruinosa* NMCCC 013. Anastomotic branched sheaths can be observed. **Fig. 8**. UV epifluorescence micrograph of *P. pruinosa* NMCCC 014 confirming rich pseudobranching and tree-like spreading of the fascicles. **Fig. 9**. Regularly coiled long fascicles in mats of *P. pruinosa* NMCCC 002. **Figs 10, 11**. Filaments embedded into very wide, gelatinous, amorphous, homogeneous, and diffluent masses of mucilage. Open screw-like left-handed helixes and fasciculated and closely entangled filaments can be observed, both embedded in the voluminous, thick mucilage. Figure 10 shows the diffluent masses of mucilage in *P. pruinosa* NMCCC 001, while **Fig. 11** depicts the masses of mucilage in *P. pruinosa* NMCCC 013. Scale bar = 10 μm. Arrows with labels: s, sheaths; oh, screw-like left-handed open helixes; pb, pseudobranching; m, mucilage.

Table 1. *Pseudanabaena* strains included in the study.

Taxon	Strain designation	Locality and habitat (coordinates)	Isolator, and year of isolation
Pseudanabaena pruinosa	NMCCC 001	Arctic, Svalbard Archipelago, central part of the Spitsbergen Island, northwest of Petuniabukta Bay, foreland of the valley-type glacier Hørbyebreen, icy microbial soil crust 78°55′51″N, 16°37′31″E	Šnokhousová & Elster, (2011)
Pseudanabaena pruinosa	NMCCC 013	Arctic, Svalbard Archipelago, central part of the Spitsbergen Island, northwest of Petuniabukta Bay, foreland of the valley-type glacier Hørbyebreen, icy microbial soil crust 78°55′54″N, 16°37′31″E	Šnokhousová & Elster, (2011)
Pseudanabaena pruinosa	NMCCC 014	Arctic, Svalbard Archipelago, central part of the Spitsbergen Island, west of Petuniabukta Bay, top of the first summit of Mumien Peak, 773 m above sea level, icy microbial soil crust 78°70′02″N, 16°31′47″E	Šnokhousová & Elster, (2011)
Pseudanabaena pruinosa	NMCCC 002	Arctic, Svalbard Archipelago, central part of the Spitsbergen Island, southeast of Petuniabukta Bay, mountain Fortet, 233 m above sea level, fast streams from melted glaciers, along with *Hydrurus foetidus*, 78°68′15″N, 16°65′55″E	Šnokhousová *et al.,* (2015)

Ultrastructure

For ultrastructural investigations, the strains were fixed in 2.5% glutaraldehyde and 4% glucose in 0.5 M phosphate buffer at pH 7.2 for 3 days at room temperature. Samples were rinsed with 0.5 M phosphate buffer with 4% glucose and post-fixed in 2% osmium tetroxide for 2 hours at room temperature. After washing with 0.5 M phosphate buffer, the cells were dehydrated through a series of isopropanol solutions and embedded in Spurr's resin (Spurr, 1969) with propylene oxide. Ultrathin sections of 60–70 nm were cut using a Leica EM UC7 ultramicrotome. The sections were stained with uranyl acetate and lead citrate and examined with a Jeol JEN 1010 transmission electron microscope at 80 kV.

Molecular analyses

Genomic DNA was isolated from the unialgal strains following a modified xanthogenate–SDS buffer extraction protocol with the addition of 3% PVPP and PEG–$MgCl_2$ precipitation (Mareš *et al.*, 2013). A section of the rRNA operon with expected amplicon length of around 1950 bp, containing the partial 16S rRNA gene and the 16S–23S internal transcribed spacer (ITS) was amplified using the primers CYA106F (CGGACGGGTGAGTAACGCGTGA, Nübel *et al.*, 1997) and 23S30R (synonym – B23S, CTTCGCCTCTGTGTGCCTAGGT, Lepère *et al.*, 2000). The PCR reaction mixture contained approximately 100 ng template DNA, 0.2 µM of each primer, 1× AmpliTaq Gold 360 Buffer (Applied Biosystems™), 0.2 mM dNTPs, 1 U AmpliTaq Gold 360 DNA Polymerase (Applied Biosystems™), 2 mM $MgCl_2$ and 5 µl 360 GC Enhancer (Applied Biosystems™) in a total volume of 25 µl. PCR amplification was performed with an initial denaturalization step (95°C, 15 min), 40 cycles of 1 min at 95°C, 40s at 59°C and 3 min at 72°C, followed by a final extension for 10 min at 72°C and cooling to 4°C. Successful PCR amplification (showing amplification products of the expected length of around 1950 bp) was confirmed by running a subsample on a 1.5% agarose gel stained with ethidium bromide. All PCR products were purified using the ExoSAP-IT™ PCR Purification Kit and then sequenced using the primers CYA106F, LPW58R (AGGCCCGGGAACGTATTCAC, Woo *et al.*, 2000), f3L (GTCCCGCAACGAGCGCAAC, Hiraishi *et al.*, 1994), and 23S30R, applying the BigDye™ Terminator v1.1 Cycle Sequencing Kit. Sequencing was performed on the 8-capillary 3500 Genetic Analyser in the Research Centre for Genetic Engineering and Biotechnology 'Georgi D Efremov', Macedonian Academy of Sciences and Arts, Skopje.

Phylogenetic analyses

Analyses of the 16S rRNA gene

The partial 16S-ITS-23S rRNA sequences were deposited in GenBank, under the following accession numbers: MT741851 (NMCCC 001), MT741852 (NMCCC 013), MT741854 (NMCCC 014) and OR897887 (NMCCC 002). A BLAST search of highly similar sequences across the major gene databases (GenBank/EMBL ENA/DDBJ) was performed, and the sequences of the 16S rRNA gene were aligned in MAFFT (mafft.cbrc.jp; Katoh *et al.*, 2002). Alignments were visually reviewed with BioEdit 7.0.1 (Hall, 1999). The 16S rRNA gene alignment contained 162 sequences with 1010 columns. The General Time-Reversible model with invariant sites and gamma distribution (GTR+I+G) was identified by the jModelTest 2 software (Darriba *et al.*, 2012) as the best nucleotide substitution model for the phylogenetic analysis, based on both the Akaike and Bayesian information criteria. This substitution model was used in the following Bayesian inference and Maximum likelihood analyses, by specifying four gamma categories, and setting the gamma shape parameter at 0.5290, in compliance with the jModelTest results.

Phylogenetic reconstruction was inferred using Bayesian inference (BI) with MrBayes 3.2.6 (Ronquist *et al.*, 2012). The BI calculation employed Metropolis-Coupled Markov Chain Monte Carlo (MCMCMC) analyses with three heated chains and one cold chain in each of two independent runs processed for 10 million generations. Tree sampling was performed every 1000 generations until the likelihood values were stabilized with an average standard deviation of split frequencies below 0.01. Burn-in of the initial 25% generations allowed stabilization of the likelihood value in the set of sampled trees, and a 50% majority-rule consensus tree with estimated posterior probabilities of branches was constructed.

Maximum likelihood analysis (ML), applying the general time-reversible model with invariant sites and gamma distribution (GTR+I+G), was used for a phylogeny reconstruction inferred by RAxML v. 8.0.0 (Stamatakis, 2014) with 1000 bootstrap replicates at the supercomputing facility of the Faculty of Sciences, University of South Bohemia. Additionally, a Neighbour-joining analysis (NJ) was conducted under a maximum composite likelihood model with uniform rates among sites in MEGA 11 (Tamura *et al.*, 2021) with 1000 bootstrap repetitions. The bootstrap values from the ML and NJ analyses were mapped onto the BI tree. The final graphical refinement of figures was made in Adobe Illustrator CS6.

Analyses of the 16S-23S rRNA internal transcribed spacer (ITS)

In the 16S-23S rRNA operon, different regions of the internal transcribed spacer (ITS) and conserved motifs were identified following Iteman *et al.* (2000); additionally, the V3 helix was identified based on Bohunická *et al.* (2011). The putative secondary structures of D1–D1′, Box B, V2 and V3 helixes were predicted using the Mfold web server version 3.2 (Zuker, 2003) with the default settings and temperature fixed at 37°C, except for the structure-drawing mode, which was set to 'Untangle with loop fix'. The secondary structures with minimum free energy (ΔG) were chosen and redrawn in Adobe Photoshop CS6.

Statistical analyses

Statistical analyses were performed in IBM SPSS Statistics® 21. The morphometric quantitative variables are reported as mean ± SD. One-way ANOVA with the Tukey HSD post-hoc test was used for the comparison of the means among the groups. In all cases, the level of statistical significance was defined as $p < 0.05$.

Results

Morphology, growth and phenotypic plasticity

Morphological evaluation of the four Arctic glacial and soil crust strains (Figs 2, 3 , 5, 10, 12, 14–16 for strain NMCCC 001; Figs 4, 9, 17–20 for strain NMCCC 002; Figs 6, 7, 11, 13, 24–26 for strain NMCCC 013; Figs 8, 21–23 for strain NMCCC 014) led to their taxonomic placement in the genus *Pseudanabaena* according to the description of Lauterborn (1915) and the later revision by Komárek & Anagnostidis (2005). The Arctic strains were compared with the strains *P. catenata* SAG 1464–1 and SAG 254.80, as well as with the strain *P. galeata* SAG 13.83, which has polar aerotopes (Table 2). All strains were characterized by thin trichomes, showing deep constrictions, with translucent, thick spaces between adjacent cells (i.e. the 'hyaline bridges' reported in Skuja (1948) and Anagnostidis (1961)), giving the appearance of 'clearly separated cells' in the trichome; this morphology fitted well with the original representation of the genus *Pseudanabaena* by Lauterborn (Lauterborn, 1915, pl. III: fig. 27). Clear differentiation of the cell contents into centroplasm and chromatoplasm was evident even in light microscopy, indicating a parietal arrangement of the thylakoids.

In terms of the morphometric features of the four strains, statistical analyses showed that, regarding trichome width, NMCCC 014 differed significantly from the other three Arctic strains (ANOVA $F = 31{,}6370$, $p < 0.001$). NMCCC 014 showed higher variability in trichome width, with some narrower individuals in the population (0.7–0.9 µm wide), which were not detected within the other Arctic strains. Regarding cell length, the strain NMCCC 001 had significantly shorter cells than the other three Arctic strains (ANOVA $F = 21{,}9487$, $p < 0.001$); the cells of this strain were almost always isodiametric.

Compared with the available strains of *P. catenata*, both SAG 254.80 (ANOVA $F = 30.1814$, $p < 0.001$) and SAG 1464–1 (ANOVA $F = 29.5062$, $p < 0.001$) showed significantly wider trichomes than NMCCC 0014, and significantly thinner trichomes than NMCCC 001. Both strains showed very significant differences in cell length when compared with all of the four Arctic strains (ANOVA $F = 132.4080$, $p < 0.00001$).

Similarly, the comparison of the available strain of *P. galeata* (SAG 13.83) with the four Arctic strains showed it had significantly thinner trichomes than NMCCC 001 (ANOVA $F = 31{,}7291$, $p < 0.001$) and significantly longer cells than all four Arctic strains and the strains of *P. catenata* (SAG 254.80 and SAG 1464–1) (ANOVA $F = 121.226$, $p < 0.00001$).

Figs 12, 13. Branched sheaths and pseudofilaments. **Fig. 12**. Details of the anastomotic branched sheaths in *Pseudanabaena pruinosa* NMCCC 001. **Fig**. **13**. Details of pseudobranched filaments with characteristic tree-like spreading forming heteropolar thallus unit in *Pseudanabaena pruinosa* NMCCC 013. Arrows with labels: abs, anastomotic branched sheaths; pb, pseudobranching. Scale bar = 10 μm.

The statistical analyses of morphometric variables indicated significantly shorter cells in the four Arctic strains than in the strains of *P. catenata* and *P. galeata*. Cells in the Arctic strains were mostly isodiametric or about 1.5 times longer than wide, with a characteristic spherical, spherical-to-quadratic or short barrel-cell shape.

Besides cell length, the four analysed strains differed from the type species *P. catenata* by the presence of aerotopes and apical cells with a single, specific, large ('galeate') aerotope (Figs 15–18, 20, 24, 28, in Figs 15–18 also indicated by an arrow 'a'), similar to *P. galeata* (Böcher, 1949). However, these strains differed from *P. galeata* and from all other described species with polar aerotopes, such as the *P. foetida* Niiyama, Tuji & Ichise species complex (Niiyama *et al.*, 2016; Tuji & Niiyama, 2016), *P. cinerea* Tuji & Niiyama (Tuji & Niiyama, 2018), *P. yagii* Tuji & Niiyama (Tuji & Niiyama, 2018), *P. amphigranulata* (Goor) Anagnostidis (Anagnostidis, 2001) and *P. biceps* (Böcher, 1946). Indeed, the four investigated strains were characterized by a distinctive moniliform outline with a string-of-beads-like trichome morphology (Figs 2–5, 7–8, 11–13, 15, 16, 18), and long trichomes with > 20 cells, which were very slightly motile. Thinner 'hyaline bridges' and deep trichome constrictions were also characteristic of the Arctic strains. Moreover, the four strains had eight phenotypic characters not previously associated with the genus *Pseudanabaena*:

(1) *Facultative, widened, and branched sheaths*: the observed sheaths (Figs 2, 5, 7, 12–13) were wide (2.1–8.6 μm), fine, colourless, with clearly observable refractive margins, usually enveloping

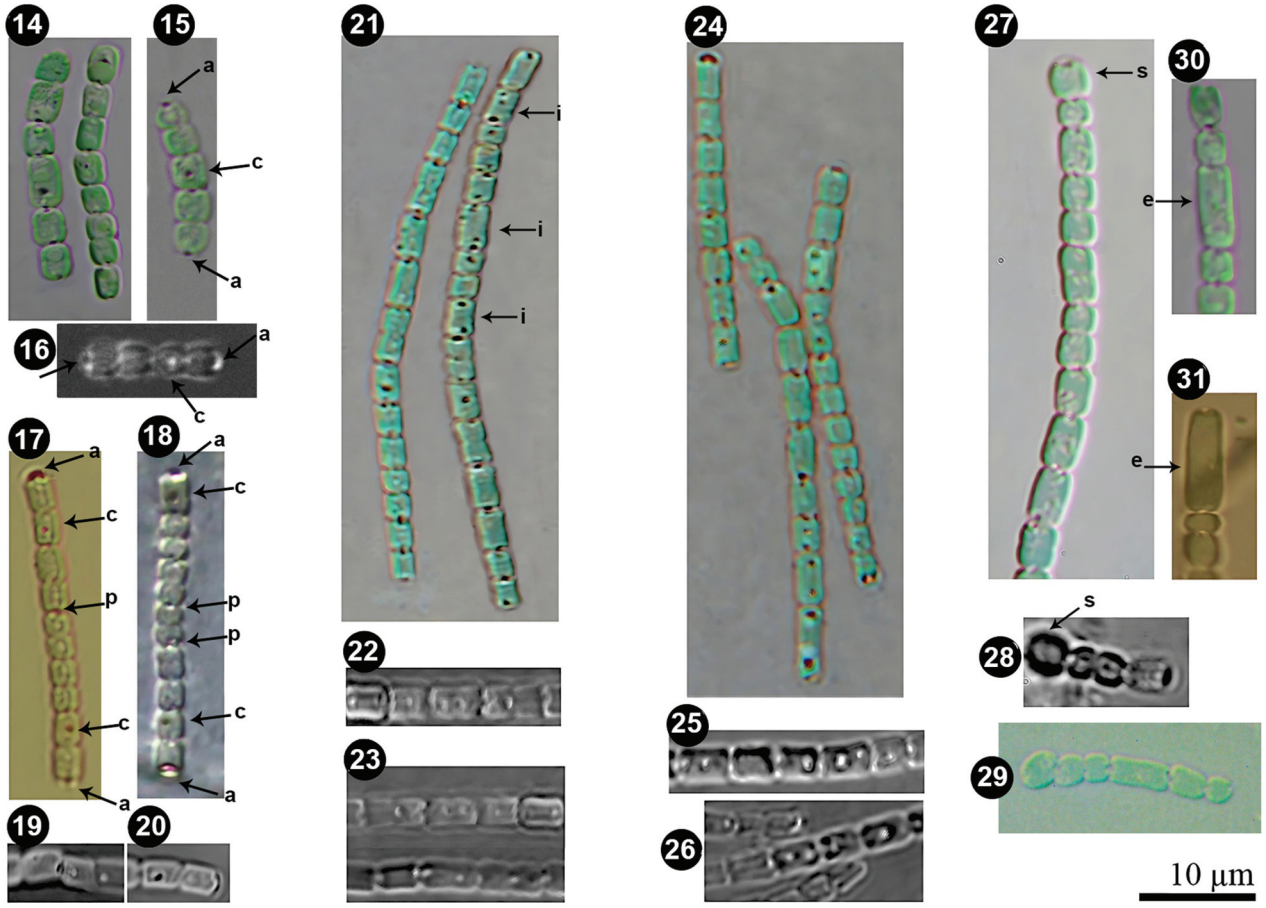

Figs 14–26. Details of polar and central aerotopes variability in *Pseudanabaena pruinosa*. **Figs 14–26**. *P. pruinosa* NMCCC 001. **Figs 17–20**. *P. pruinosa* NMCCC 002. **Figs 21–23**. *P. pruinosa* NMCCC 014. **Figs 24–26**. *P. pruinosa* NMCCC 013. **Figs 27–29**. Presence of swollen cells in *P. pruinosa* NMCCC 001 (**Fig. 27**), NMCCC 002 (**Fig. 28**) and NMCCC 013 (**Fig. 29**). **Figs 30, 31**. Irregular cell division and presence of elongated cells in *P. pruinosa* NMCCC 013 (**Fig. 30**) and NMCCC 002 (**Fig. 31**). Arrows in **Figs 15–18** indicate apical cell aerotopes (designated with a), central aerotopes (c) and polar aerotopes (p). Arrows in **Fig. 21** indicate cells with an irregular position of aerotopes. Arrows in **Figs 27, 28** indicate swollen cells (s), and arrows in **Figs 30, 31** indicate elongated cells (e). Scale bar = 10 µm.

several bundled trichomes into a single filament. Sheaths could be branched (Fig. 12).

(2) *Heteropolar filaments*, i.e. curved and flexible filaments containing many closely entangled and fasciculated trichomes at the base, and a few or solitary trichomes in the apical part of the single sheath (Figs 2, 5, 7). This character was very similar to the concept of the heteropolar filaments in *Schizothrix fasciculata* Gomont ex Gomont (compare with fig. 400 in Komárek & Anagnostidis, 2005).

(3) *Presence of divaricated, richly pseudobranched filaments* due to the presence of anastomosed branched sheaths, resulting in *apparent branching of* the filaments, forming heteropolar units with a base and wide apical part within the thallus (Figs 5, 7, 8, 13). Up to now, *Pseudanabaena* has been considered not to exhibit false branching (Komárek & Anagnostidis, 2005).

(4) *Pseudobranched filaments embedded in thick masses of voluminous amorphous mucilage*: the tree-like pseudobranched filaments were structured and embedded into very wide, gelatinous, amorphous, homogeneous masses of mucilage, clearly observed by LM (Figs 10–11, indicated by arrow and m).

(5) *Presence of both polar and central aerotopes* (Figs 14–26; in Figs 15–18 *polar and central aerotopes indicated by arrows*), *and some irregular aerotopes throughout the cell* (Fig. 21, indicated by arrows).

(6) *Presence of distinct and very characteristic regularly coiled voluminous screw-like helixes embedded in the thick mucilage* (Figs 6, 10). Their frequent appearance is shown in Supplementary fig. S1.

(7) *Ability to produce swollen cells* (Figs 27–29) *and to undergo irregular cell division resulting in elongated cells* in unfavourable conditions

Table 2. Morphological evaluation of the Arctic strains NMCCC 001, NMCCC 002, NMCCC 013, NMCCC 014, and their comparison with the strains designated as *Pseudanabaena catenata* and *P. galeata* in culture collections.

Characters	*P. pruinosa* NMCCC 001	*P. pruinosa* NMCCC 002	*P. pruinosa* NMCCC 013	*P. pruinosa* NMCCC 014	*P. galeata* SAG 13.83	*P. catenata* SAG 1464–1	*P. catenata* SAG 254.80
Trichome width (μm)	1.5–2.4 **1.8 ± 0.2**	1.4–2.4 **1.6 ± 0.1**	1.2–1.9 **1.5 ± 0.2**	0.7–1.8 **1.2 ± 0.4**	1.1–1.7 **1.3 ± 0.1**	1.4–1.9 **1.6 ± 0.1**	1.3–1.8 **1.5 ± 0.1**
Cell length (μm)	1.2–2.4 **1.8 ± 0.4**	1.5–3.5 **2.3 ± 0.5**	1.8–2.7 **1.9 ± 0.7**	1.6–2.8 **2.0 ± 0.5**	3.5–7.8 **5.4 ± 1.1**	3.2–8.9 **5.4 ± 0.9**	2.8–7.1 **4.7 ± 0.7**
Length: Width ratio	Isodiametric **1-fold ± 0.2**	Mostly 1.5× longer **1.6-fold ± 0.4**	Mostly isodiametric to 1.5× longer **1.5-fold ± 0.5**	Mostly 1.5× longer **1.6-fold ± 0.7**	Mostly 4× **4.0-fold ± 0.8**	Mostly 3× **3.4-fold ± 0.7**	Mostly 3× **3.0-fold ± 0.8**
Cell shape	Spherical	Spherical to barrel-shaped	Spherical to quadratic	Quadratic to mostly barrel-shaped	Long cylindrical with rounded ends	Cylindrical with rounded ends	Cylindrical with rounded ends
Cell colour	Blue-green to vivid green	Brownish to violet	Pale blue-green to vivid green	Pale green, pale blue-green	Blue-green to vivid green	Blue-green to vivid green	Blue-green to vivid green
Sheaths	Facultative, widened and branched	Facultative, widened and branched	Facultative, widened and branched	Facultative, widened and branched	No	No	No
'Hyaline bridges'	Thin	Thin	Thin	Thin	Thick and evident	Thick and evident	Thick and evident
Constrictions	Intensively deep	Intensively deep	Distinct	Distinct	Slightly to evidently	Distinct	Distinct
Aerotopes	Polar and central	Polar and central	Polar and central	Polar and central	Only polar	Absent	Absent
Granules	Only minute	Rarely, small	Rarely, small	Facultative	Rarely, small	Prominent	Prominent
Motility	Very slightly	Slightly	Very slightly	Slightly	Quite motile	Motile	Motile

Note: Clearly elongated cells resulting from irregular cell division (Figs 30, 31) were not included in the measurements. n = 100 (i.e. for each strain, 100 cells were analysed).

(details of conditions given below) (Figs 30–31).

(8) *Formation of oval voluminous balls by thallus* (not shown).

Since no *Pseudanabaena* species has hitherto been reported to have the ability to produce sheaths (especially branched sheaths with pseudobranched filaments) or heteropolar filaments, to undergo irregular cell division, and to produce central aerotopes, these features, observed for the four investigated strains, suggest that they differ from all described species of *Pseudanabaena*.

The four Arctic strains were shown to be psychrotrophic according to the currently accepted definitions of psychrophilic, psychrotrophic and psychrotolerant species (Morita, 1975). The organisms were able to grow at 4°C and all of them showed an optimal growth temperature of 15°C (Table 3). However, they were not psychrophilic, since they were able to grow at temperatures slightly above 20°C (22°C). The strains were not able to grow at temperatures ≥ 25°C unlike psychrotolerant cyanobacteria and these temperatures caused very fast decay of the thalli, resulting in a yellow, turbid suspension. Their specific growth rates after 7 days at different temperatures are given in Table 3. Statistical analyses have confirmed highly significant differences in growth rates among the four different temperature conditions ($p < 0.001$).

In terms of their phenotypic plasticity, a higher light intensity (83 μmol $m^{-2}s^{-1}$) resulted in slightly longer cells (4–6 μm) and presence of more frequent and larger aerotopes. Temperatures below 15°C resulted in shorter cells and fewer aerotopes; in contrast, at > 15°C, higher phenotypic plasticity of trichome width and cell length was observed (different trichomes had different widths in the same culture, and cells with different sizes were observed in the same trichome), with the occurrence of irregular cell division, resulting in some clearly elongated cells (> 6 μm long; Figs 27, 28), or swollen cells (Fig. 26). Temperatures >20°C and prolonged growth over the stationary phase (usually after 3 months of cultivation in 60 ml liquid Z8 medium) both resulted in observable intense irregular cell division, mainly longer cells (4–6 μm long), clearly elongated cells (> 6 μm long) and swollen cells (2.5–3.4 μm wide).

Ultrastructure

Ultrastructural analyses (Figs 32–37) confirmed that all four Arctic strains had characters congruent with those reported by Guglielmi & Cohen-Bazire (1984) for the genus *Pseudanabaena*. In particular, all the analysed strains had parietal thylakoids, with 5–8 concentric thylakoid membranes parallel to the cell wall; 4–6 times thicker murein layers at the partitions between adjacent cells compared with parietal peptidoglycan (Figs 35, 37); and deep constrictions. Clusters of gas vacuoles (grouped as polar and central aerotopes) were confirmed for each of the strains.

Table 3. Specific growth rates of *Pseudanabaena* species after 7 days (μ_7) at different temperatures. The given values for each strain represent means from five replicates. The overall mean ± SD for each temperature condition was calculated based on all values from the five replicates of the experiment.

Strains	4°C	8°C	15°C	22°C	25°C
P. pruinosa NMCCC 001	0.20 ± 0.04	0.22 ± 0.01	0.40 ± 0.01	0.26 ± 0.02	yellow decay
P. pruinosa NMCCC 002	0.07 ± 0.03	0.19 ± 0.01	0.37 ± 0.02	0.22 ± 0.03	yellow decay
P. pruinosa NMCCC 013	0.14 ± 0.02	0.21 ± 0.01	0.41 ± 0.02	0.27 ± 0.02	yellow decay
P. pruinosa NMCCC 014	0.12 ± 0.05	0.21 ± 0.01	0.36 ± 0.01	0.22 ± 0.02	yellow decay
Mean ± SD	**0.13 ± 0.05**	**0.21 ± 0.01**	**0.39 ± 0.02**	**0.24 ± 0.03**	

Phylogenetic analyses based on the 16S rRNA gene and genotypic characters

The phylogenetic tree based on 16S rRNA (Fig. 38) shows the position of *Pseudanabaena* sensu stricto (shaded in grey) within the Cyanobacteria, indicating that its closest relationship is with the recently established family Thalassoporaceae, together forming the order Pseudanabaenales. The genus *Pseudanabaena* and the order Pseudanabaenales were related to the simplest cyanobacterial lineages (Thermostichales, Gloeobacteriales) according to the 16S rRNA data. This was congruent with the phylogenomic tree provided by Strunecky *et al.* (2023). The position of the order Pseudanabaenales and its relationship to the rest of the phylum Cyanobacteria (Thermosynechococcaceae, Oculatellales, Nodosilineales, Synechococcales, Oscillatoriaceae, Chroococcaceae, Microcoleaceae, Nostocales and others) can also be inferred from the tree.

The four Arctic strains shared > 99% 16S rRNA sequence identity and in the phylogenetic tree (Fig. 38), they grouped together within the *Pseudanabaena sensu stricto* cluster, forming a compact clade (clade A) that was clearly separated from the other *Pseudanabaena* species clades.

The 16S rRNA gene sequence (sequence accession: MT741851) of NMCCC 001, reference strain of clade A, showed the highest identity with the 16S rRNA of other *Pseudanabaena* strains isolated from similar extreme ecological conditions, such as the Canadian strains misidentified as '*Pseudanabaena frigida*' (i.e. the Arctic strain ULC067, isolated from Bylot Island, sequence accession: MH118734, identity: 99.5%; the sub-Arctic strain ULC069, sequence accession: MH118736, identity: 99.6%), as well as a strain isolated from cryptobiotic soil crusts (*Pseudanabaena* sp. UMPCCC 1113, sequence accession: KM218875; identity: 99.5%). Concerning the data from uncultured cyanobacteria, the reference strain of clade A – NMCCC 001 showed the highest similarity to cyanobacteria growing underneath snow, such as uncultured samples isolated from subnival alpine soils in the high Himalayas (sequence accessions: HQ189020, HQ189113 and HQ188983, identity: 99.6%), as well as with uncultured bacteria isolated from glaciers in China, including PCR.UMS3_21

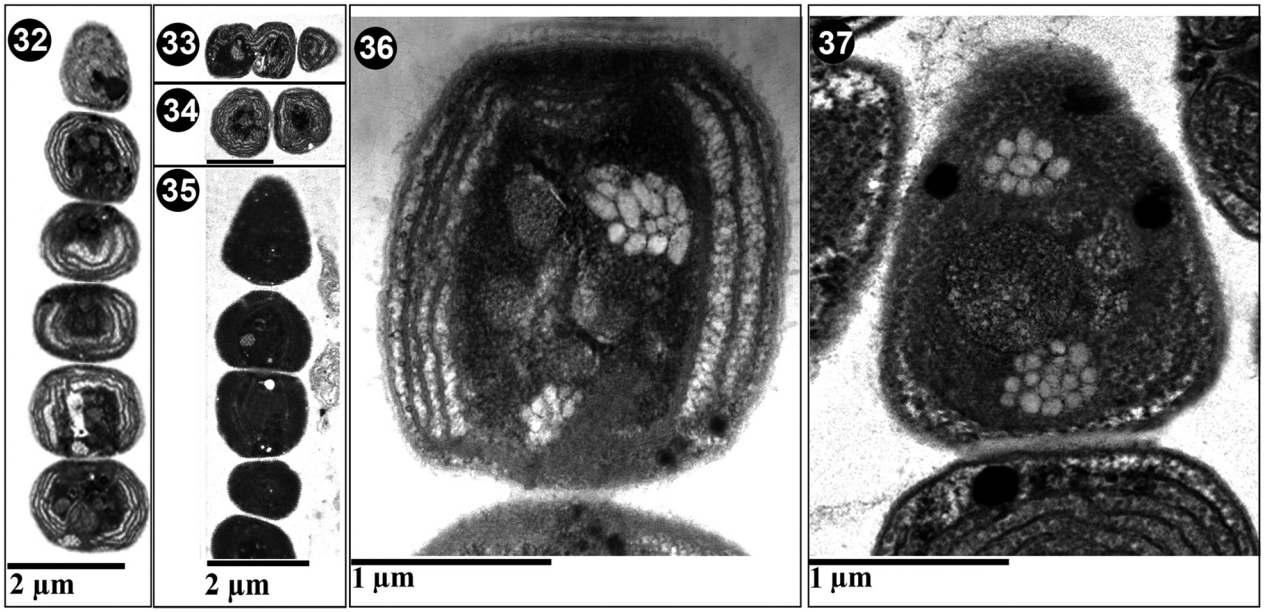

Figs 32–37. Ultrastructure of *Pseudanabaena pruinosa*. **Fig. 32**. *P. pruinosa* NMCCC 001. The parietal organization of 5–8 thylakoid membranes can be observed, as well as the position of polar aerotopes. **Fig. 33**. Central aerotopes in *P. pruinosa* NMCCC 001. **Fig. 34**. Cell shape and ultrastructure of *P. pruinosa* NMCCC 002. **Fig. 35**. *P. pruinosa* NMCCC 013. The parietal organization of thylakoids and the presence of a central aerotope can be observed. **Fig. 36**. Polar and central aerotopes in *P. pruinosa* NMCCC 013. **Fig. 37**. Aerotopes with irregular position within the cell of *P. pruinosa* NMCCC 014. Scale bar = 10 µm.

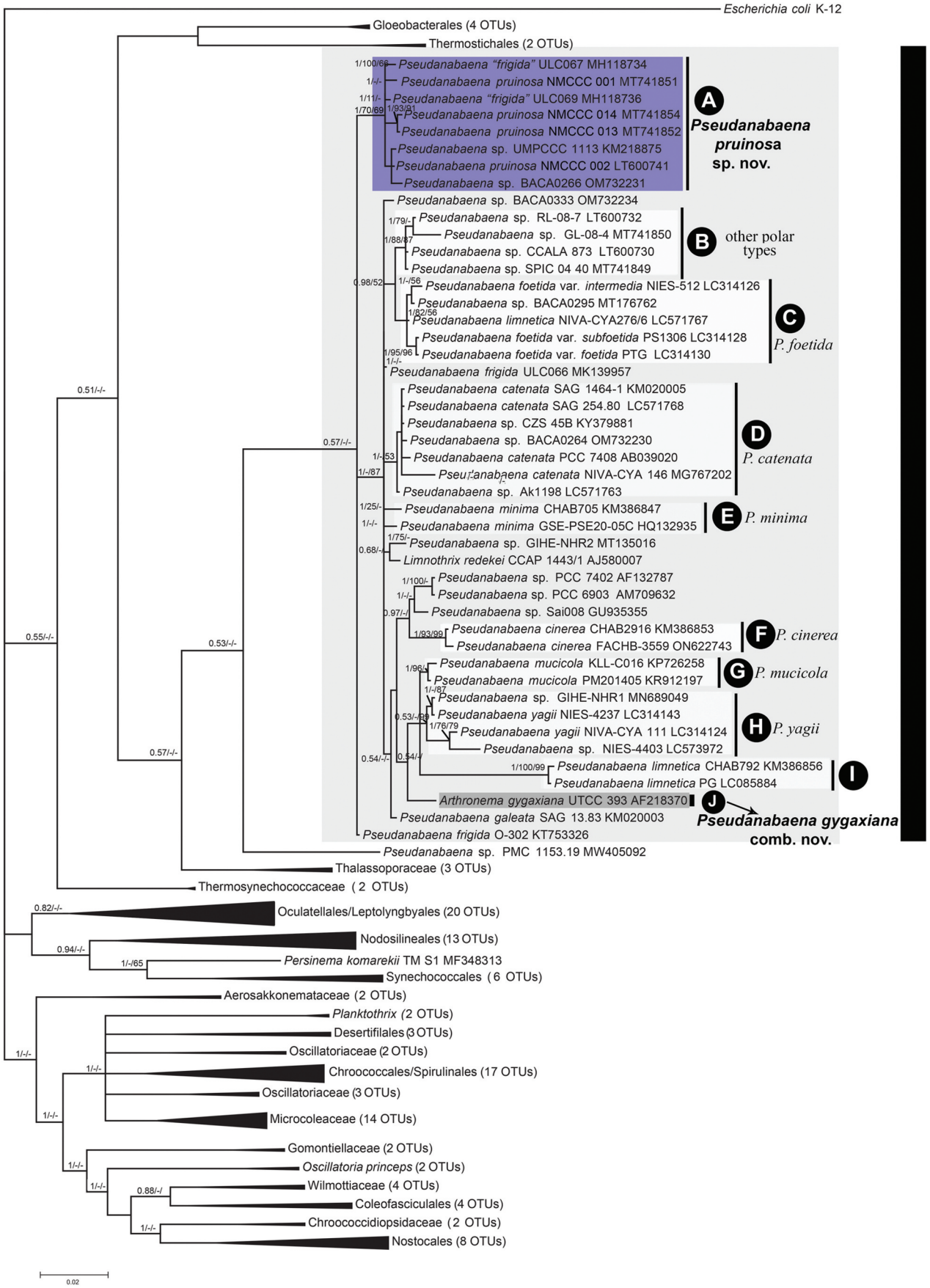

Fig. 38. Phylogenetic analysis based on 162 sequences of 16S rRNA gene showing the position of the *Pseudanabaena* species. The phylogenetic tree topology was based on Bayesian inference, and the tree was validated by Maximum likelihood (GTR+Γ+I model) and Neighbour-joining analysis. Branch support values are shown as Bayesian posterior probability/Maximum likelihood bootstrap support/Neighbour-joining bootstrap support values, respectively. Values < 0.5 or 50% are not shown. Vertical bars represent clades that correspond to the different *Pseudanabaena* infrageneric units.

(sequence accession: LC104280, identity: 99.3%), OTU5 (sequence accession: LC103279, identity: 99.5%) and Qiyi-cya-OTU7 (sequence accession: AB569632, identity: 99.6%). Besides the above-mentioned sequences, the other sequences in GenBank showed ≤ 98.5% identity with NMCCC 001 (Table 4).

Besides clade A, the 16S rRNA phylogenetic tree (Fig. 38) showed that the genus *Pseudanabaena* is diversified into several infrageneric units, with some units forming recognizable clades (indicated as clades A–J), that correspond to different *Pseudanabaena* species (i.e. *P. foetida, P. catenata, P. minima, P. cinerea, P. mucicola* (Naumann & Huber-Pestalozzi) Schwabe, *P. yagii, P. limnetica* and others), defined according to traditional cytomorphological characters. Clade A was well-defined with high bootstrap support, clearly separated and distant from the clades of other *Pseudanabaena* species with similar characteristics, i.e. the ability to produce polar aerotopes and special apical cells equipped with a large, 'galeate' aerotope (*P. galeata, P. foetida, P. cinerea* and *P. yagii*). The strains in clade A were distant from the other *Pseudanabaena* strains isolated from Svalbard (clade B, i.e. strains CCALA 873 and SPIC_04_40 from Hornsund, Kvartsittoden, which were grouped with strains RL-08-7 and GL-08-4 from Antarctica). Clade A strains were especially distant from the 16S rRNA of *Stenomitos frigidus* (F.E.Fritsch) Miscoe & J.R.Johansen (basionym: *Phormidium frigidum* Fritsch 1912, later homotypic synonyms ≡ *Leptolyngbya frigida* (Fritsch) Anagnostidis 1988, along with the concept of ≡ *Pseudanabaena frigida* (Fritsch) Anagnostidis, 2001), with 88.8% identity between the sequences of strain NMCCC 001 and strain CANT10 (Table 4) of *Stenomitos frigidus*.

Analyses of the 16S-23S rRNA internal transcribed spacer (ITS)

The analysis of the 16S-23S ITS region in the four Arctic strains and the other *Pseudanabaena* strains included in this study (Fig. 38) with available ITS sequences showed that this region contains both $tRNA^{Ile}$ and $tRNA^{Ala}$ sequences in its structure, separated by the variable V2 stem. The section of the ITS containing $tRNA^{Ile}$, V2 and $tRNA^{Ala}$ in the reference strain NMCCC 001 is shown in Fig. 39. The secondary structure of $tRNA^{Ile}$ differed from *P. cinerea*, but was similar to the *P. foetida* 16S operon, while $tRNA^{Ala}$ in NMCCC 001 and *P. cinerea* shared the same structure, but differed from *P. foetida* (secondary structures compared with Tuji & Niiyama, 2016, 2018; Figs 3 & 4).

The D1 region of the four Arctic strains was precisely 64 nt (nucleotides) long (Fig. 40), in contrast to all other analysed *Pseudanabaena* strains, which were 63 nt long (Fig. 41). The primary structure and the putative secondary structure of the D1-D1' helix of the Arctic strains were also unique and very characteristic, with two loops on the upper terminal part (one asymmetric subterminal loop, a 2-residue stem and a 6-residue terminal hairpin: Fig. 40). This structure was slightly similar only to the D1 region of *Pseudanabaena foetida* var. *subfoetida* PS1306, and *Pseudanabaena galeata* SAG 13.83 based on its outline (Fig. 41), but it differed clearly in the structure of the subterminal asymmetric loop which in the Arctic strains was smaller, composed of 7 residues, in contrast to the other two *Pseudanabaena* strains that had a 9-residue long hairpin. As far as we know, the 64 nt D1 region with a 7-residue asymmetric subterminal loop in its secondary structure is a unique feature of the Arctic strains, not present in other *Pseudanabaena* strains.

In contrast to the D1 region, the V2 helices in *Pseudanabaena* were highly variable both in terms of their length and their putative secondary structure. The V2 helix of NMCCC 001 was slightly different from the other three examined strains. Both structures (of NMCCC 001, and of the other three strains NMCCC 002/013/014, Fig. 42) had a 3 bp basal stem, a 12 nt symmetrical internal loop and 10 bp stem region. The two helices differed in the primary structure of the 10 bp stem, and in the terminal hairpin, which in NMCCC 001 had 5 residues, and in the other three Arctic strains had 4 residues. Nevertheless, both putative secondary structures were evidently different from the V2 helices of the other *Pseudanabaena* strains (Fig. 43).

Box B helices were also variable among *Pseudanabaena* strains. NMCCC 001 and NMCCC 014 had a specific putative secondary structure of their Box B helix (Fig. 44) different from all of the other *Pseudanabaena* strains (Fig. 45). Nevertheless, the other two Arctic strains (NMCCC 002 and NMCCC 013) exhibited a different Box B region, in terms of length and primary and secondary structure. The putative secondary structure of these two strains was almost identical to the Box B secondary structure of *P. catenata* SAG 1464–1, differing only in the primary structure at positions 20 and 31.

The V3 region was less informative for *Pseudanabaena*. The four analysed strains, as well as several other *Pseudanabaena* species (Figs 46–49), shared the same primary and secondary structure of the identified 12 bp long region.

Discussion

This paper focuses on the characterization of four psychrophilic *Pseudanabaena* strains (NMCCC 001,

Table 4. 16S rRNA gene sequence identity of *Pseudanabaena pruinosa* with other species of *Pseudanabaena* and related genera. Sequence identity analyses were conducted on a 1046 bp fragment of the 16S rRNA gene starting from the CTCTTTT sequence (located 55 bp downstream of the conserved GGGGAATTTTCCGCAATGGG sequence at position 359 after *Escheria coli* numbering) up to the conserved sequence GGGGTGAAG near the end of the 16S rRNA gene.

		1	2	3	4	5	6	7	8	9	10	11	12	13	14	15
1	*Pseudanabaena pruinosa* NMCCC 001 MT741851	ID	99.5%	98.2%	98.4%	98.1%	98.0%	97.3%	97.2%	98.3%	96.9%	97.8%	93.7%	89.3%	90.6%	88.8%
2	*Pseudanabaena* '*frigida*' ULC067 MH118734	99.5%	ID	98.6%	98.8%	98.6%	98.1%	97.8%	97.3%	98.0%	97.3%	98.0%	93.8%	89.5%	90.4%	88.9%
3	*Pseudanabaena catenata* SAG 1464–1 KM020005	98.2%	98.6%	ID	99.2%	98.6%	98.2%	97.9%	97.4%	97.9%	98.1%	98.6%	93.9%	88.9%	89.9%	89.4%
4	*Pseudanabaena minima* CHAB705 KM386847	98.4%	98.8%	99.2%	ID	98.6%	98.2%	98.1%	97.6%	97.9%	97.6%	98.4%	94.0%	89.3%	90.3%	89.3%
5	*Pseudanabaena galeata* SAG 13.83 KM020003	98.1%	98.6%	98.6%	98.6%	ID	99.1%	98.8%	98.4%	98.8%	98.4%	98.5%	95.2%	89.0%	89.8%	89.4%
6	*Pseudanabaena* sp. CCALA 873 LT600730	98.0%	98.1%	98.2%	98.2%	99.1%	ID	98.3%	97.7%	98.9%	97.7%	97.9%	94.6%	89.2%	89.4%	89.1%
7	*Pseudanabaena mucicola* KLL-C016 KP726258	97.3%	97.8%	97.9%	98.1%	98.8%	98.3%	ID	98.9%	97.8%	98.2%	98.3%	95.0%	89.6%	89.9%	89.4%
8	*Pseudanabaena yagii* NIVA-CYA111 LC314124	97.2%	97.3%	97.4%	97.6%	98.4%	97.7%	98.9%	ID	97.6%	97.8%	97.9%	94.5%	89.7%	89.9%	89.6%
9	*Pseudanabaena foetida* var. *foetida* PTG LC314130	98.3%	98.0%	97.9%	97.9%	98.8%	98.9%	97.8%	97.6%	ID	97.3%	97.6%	94.5%	89.0%	89.8%	89.0%
10	*Pseudanabaena cinerea* CHAB2916 KM386853	96.9%	97.3%	98.1%	97.6%	98.4%	97.7%	98.2%	97.8%	97.3%	ID	97.7%	95.0%	89.2%	89.9%	88.6%
11	*Arthronema gygaxiana* UTCC 393 AF218370	97.8%	98.0%	98.6%	98.4%	98.5%	97.9%	98.3%	97.9%	97.6%	97.7%	ID	94.5%	89.2%	90.0%	90.1%
12	*Pseudanabaena limnetica* CHAB792 KM386856	93.7%	93.8%	93.9%	94.0%	95.2%	94.6%	95.0%	94.5%	94.5%	95.0%	94.5%	ID	88.1%	88.6%	88.5%
13	*Pseudanabaena* sp. PMC 1153.19 MW405092	89.3%	89.5%	88.9%	89.3%	89.0%	89.2%	89.6%	89.7%	89.0%	89.2%	89.2%	88.1%	ID	89.4%	86.7%
14	*Thalassoporum komareki* TAU-MAC 1515 MN833625	90.6%	90.4%	89.9%	90.3%	89.8%	89.4%	89.9%	89.9%	89.8%	89.9%	90.0%	88.6%	89.4%	ID	89.0%
15	*Stenomitos frigidus* CANT10 MG641934	88.8%	88.9%	89.4%	89.3%	89.4%	89.1%	89.4%	89.6%	89.0%	88.6%	90.1%	88.5%	86.7%	89.0%	ID

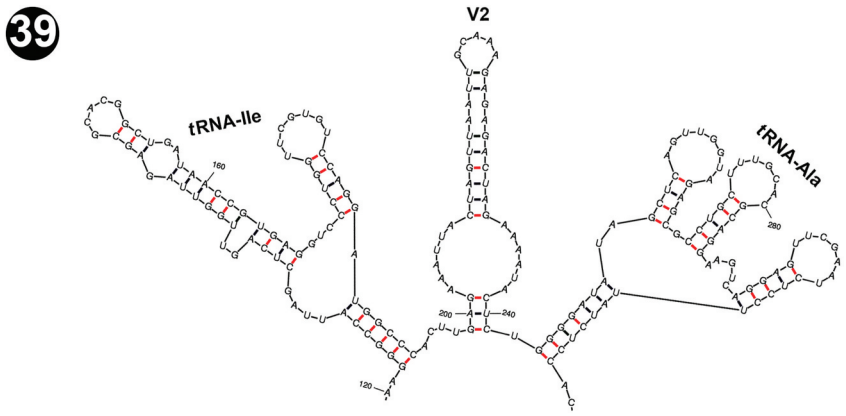

Fig. 39. Putative secondary structure of $tRNA^{Ile}$, the V2 stem and $tRNA^{Ala}$ within the 16S-23S internal transcribed spacer (ITS) of the reference strain NMCCC 001 of *Pseudanabaena pruinosa*.

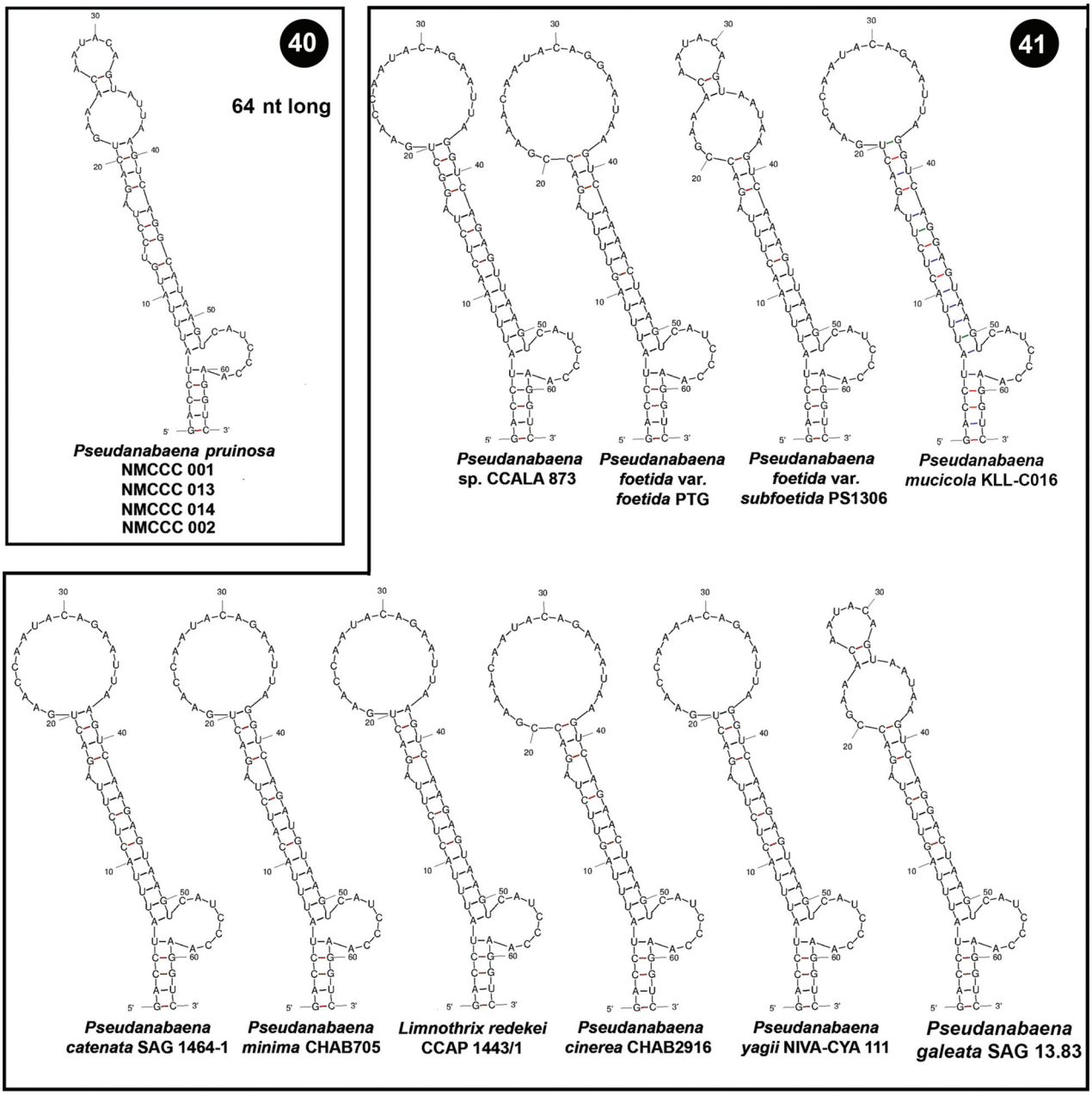

Figs 40, 41. Putative secondary structures of the conserved D1-D1' helices of the 16S–23S internal transcribed spacer (ITS) containing both tRNA genes. **Fig. 40**. *Pseudanabaena pruinosa* strains. **Fig. 41**. Other *Pseudanabaena* strains.

NMCCC 002, NMCCC 013 and NMCCC 014) isolated from extreme environments of freezing temperatures at Petuniabukta Bay (Billefjorden, Svalbard) from hydro-terrestrial and terrestrial ecosystems and growing in icy microbial soil crusts. Besides their unique ecology, the 16S rRNA phylogenetic analyses showed that these strains form a monophyletic clade (Fig. 38, clade A) which is unambiguously separated from the other *Pseudanabaena* infrageneric units, showing < 98.5% 16S rRNA sequence identity with the other *Pseudanabaena* strains available in GenBank (Table 4), and possessing a unique structure of the D1 region of its ITS. Based on these features, as well as the unusual ecology, the clade including the four investigated strains (clade A) is here designated as a new species, *Pseudanabaena pruinosa* sp. nov. Aleksovski, Krstić, Komárek & Strunecký. It is important to emphasize that this new species can be morphologically identified by light microscopy by several apomorphic traits, discussed in the following paragraphs.

The ability of *P. pruinosa* to produce sheaths entangling several trichomes is a unique trait among Pseudanabaenaceae; in fact, the subfamily Leptolyngbyoideae was first separated from Pseudanabaenaceae by Anagnostidis & Komárek (1988), and later by Komárek *et al.* (2014), as the separate family Leptolyngbyaceae, based on the presence of sheaths. Up to now, only three species of *Pseudanabaena* have been reported to possess sheaths: *P. persicina* (Reinke ex Gomont)

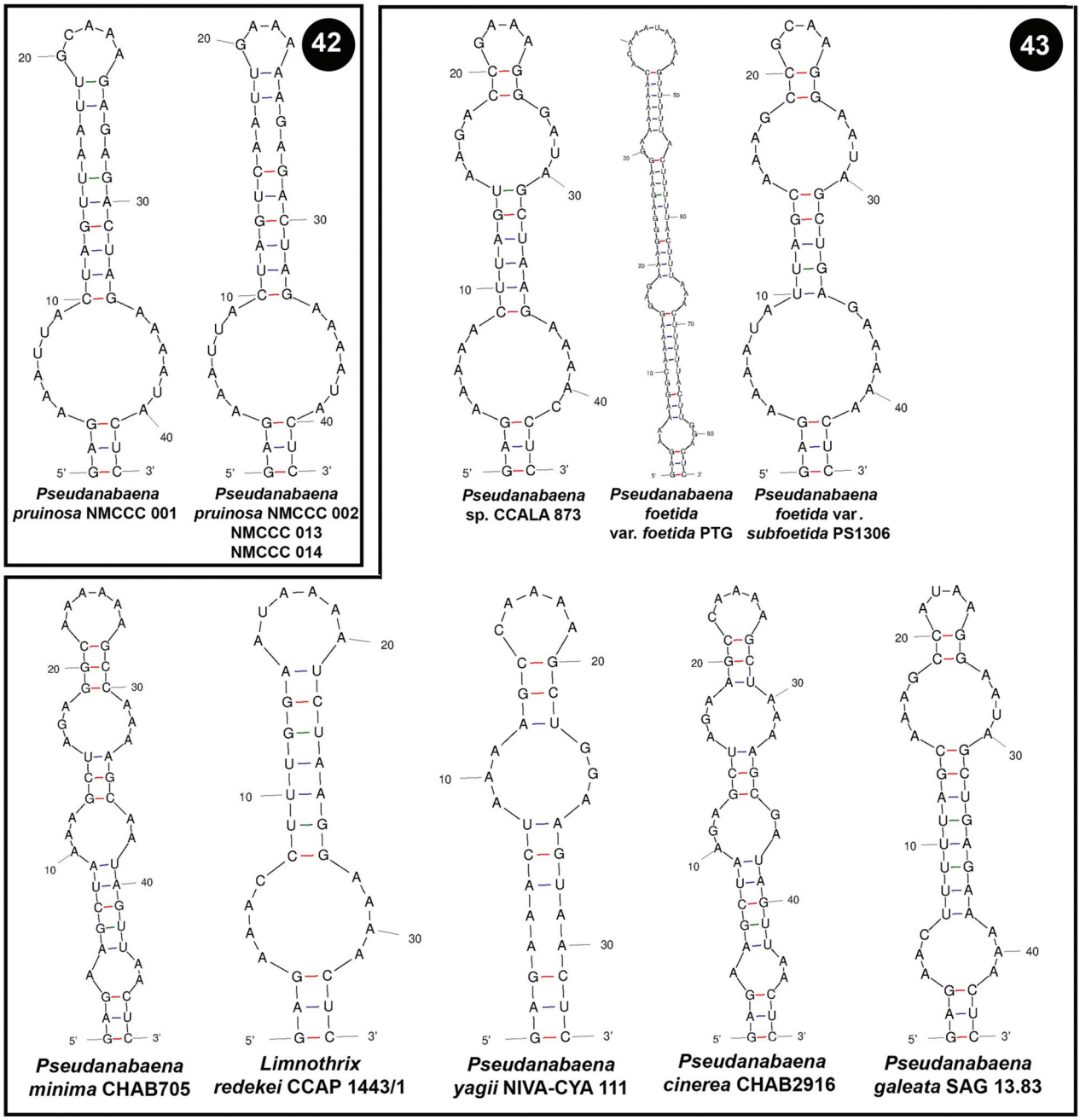

Figs 42, 43. Putative secondary structures of the V2 helices of the 16S–23S internal transcribed spacer (ITS) containing both tRNA genes. **Fig. 42**. *Pseudanabaena pruinosa* strains. **Fig. 43**. Other *Pseudanabaena* strains.

Anagnostidis and *P. spelaea* Anagnostidis, which do not have clear taxonomic status and possibly belong to Leptolyngbyaceae (Komárek & Anagnostidis, 2005), and *P. yagii*, described as occasionally possessing sheaths (Tuji & Niiyama, 2018).

Filaments living embedded in a thick and voluminous, amorphous mucilage is an interesting trait of *P. pruinosa*. Excluding the endogloeic types (which live scattered in the host's mucilage of other organisms), only a small number of *Pseudanabaena* species are reported to have the ability to produce their own mucilage, such as *P. curta* Hollerbach Cronberg & Komárek (of unresolved taxonomic and nomenclatural status) and *P. dictyothalla* (Skuja) Anagnostidis. These two species were described with wide, fine, diffluent mucilaginous envelopes, but their correct taxonomic affiliation needs to be resolved (Komárek & Anagnostidis, 2005).

The ability to produce both polar and central aerotopes is clearly an autapomorphic trait of *P. pruinosa*. The genus *Limnothrix* Meffert has been separated from *Pseudanabaena* mostly by the ability to form both polar and central aerotopes (discussed in detail in Meffert, 1987, 1988) whereas *Pseudanabaena* was supposed not to have central aerotopes (Komárek & Anagnostidis, 2005). Moreover, the absence of irregular aerotopes throughout the cell was considered an important trait for Pseudanabaenaceae, with gas vesicles always

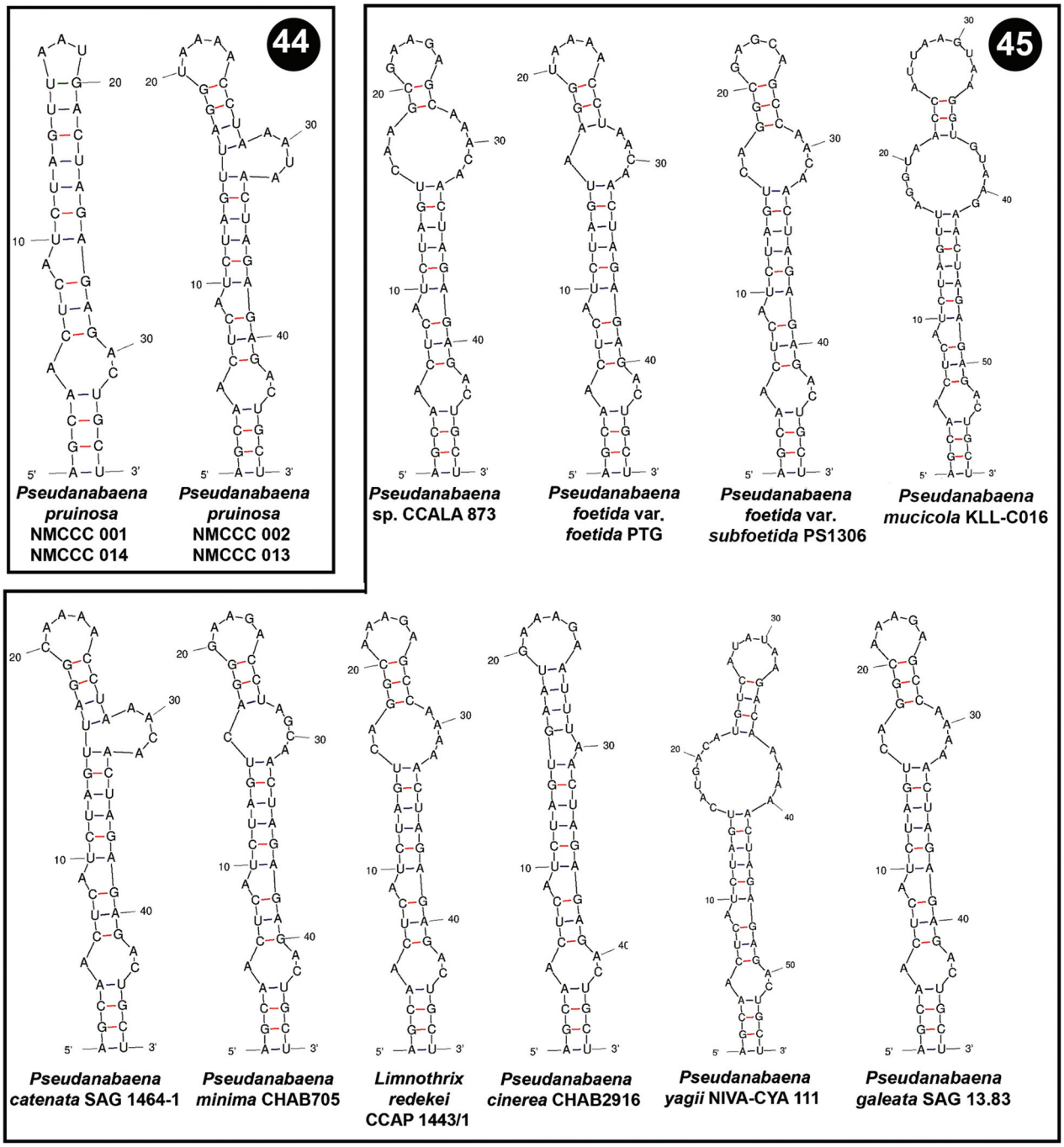

Figs 44, 45. Putative secondary structures of the Box B helices of the 16S–23S internal transcribed spacer (ITS) containing both tRNA genes. **Fig. 44**. *Pseudanabaena pruinosa* strains. **Fig. 45**. Other *Pseudanabaena* strains.

grouped in polar (*Pseudanabaena*) or both polar and central positions (*Limnothrix*) in the cell (Komárek & Anagnostidis, 2005). *P. pruinosa* is the first species in the Pseudanabaenaceae demonstrated to create irregularly distributed aerotopes within the cell.

The regularly coiled voluminous screw-like left-handed helices of *P. pruinosa* trichomes seem to be a unique phenotypic trait; such screws are characteristic of planktic species of *Arthrospira* Stizenberger ex Gomont (Gomont, 1892), but similar morphological structures have not been reported to be embedded in thick mucilage in any homocytic cyanobacteria (Komárek & Anagnostidis, 2005).

Producing swollen cells and undergoing irregular cell division are considered as apomorphic traits of the genus *Arthronema* Komárek & Lukavský (Komárek & Lukavský, 1988). Nevertheless, these morphological characters were detected in *P. pruinosa*, making it phenotypically similar to *A. gygaxiana* Casamatta & Johansen (Casamatta *et al.*, 2005).

Nevertheless, it should be stressed that *Pseudanabaena* species can show high phenotypic plasticity (especially in cell dimensions and shape) when cultivated *in vitro* and exposed to different temperatures or photoperiods (Khan *et al.*, 2018);

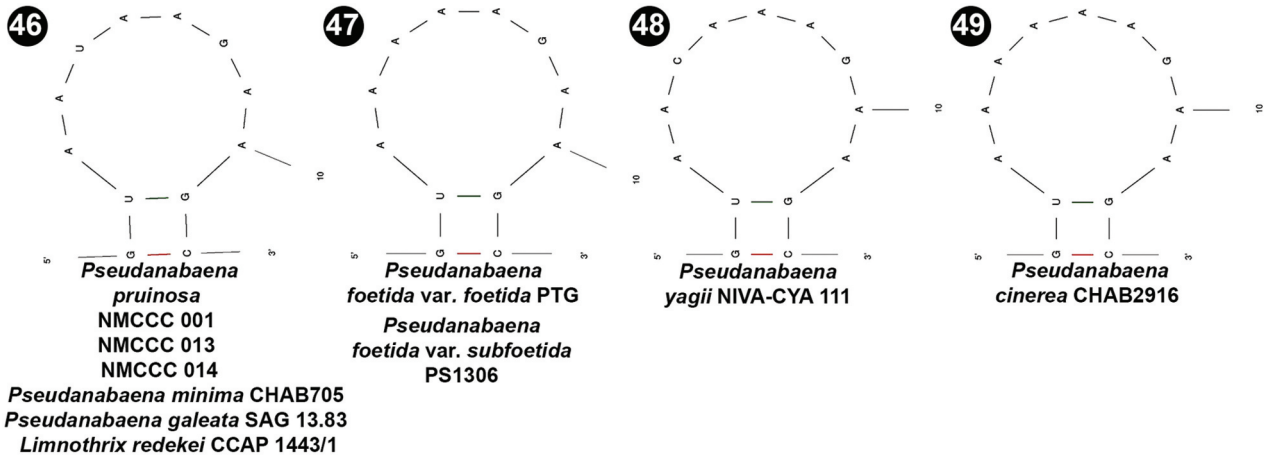

Figs 46–49. Putative secondary structures of the V3 helices of the 16S-23S internal transcribed spacer (ITS) containing both tRNA genes in *Pseudanabaena pruinosa* and other *Pseudanabaena* strains.

other phenotypic traits can change due to prolonged cultivation (e.g. loss of toxicity, Garcia *et al.*, 2017). For instance, Khan *et al.* (2017) documented significant morphological variation of the polar strain USMAC16 of *P. catenata* (isolated from Svalbard) during its adaptation to different culture conditions *in vitro*.

We have also noticed that, under specific culture conditions (i.e. cultivation at stationary phase and at temperatures higher than 15°C), *P. pruinosa* strains can show morphological variation, such as more intense irregular cell division and more elongated cells, or less conspicuous constrictions; the presence of aerotopes, especially central aerotopes, can be reduced or absent under conditions of lower light. The sheaths, as a facultative character, can be absent in *P. pruinosa*. When *P. pruinosa* has some elongated cells and/or does not show sheaths and central aerotopes, it may be confused with other *Pseudanabaena* organisms with polar aerotopes and a large 'galeate' aerotope on the apical cell. Since *P. galeata*, the *P. foetida* species complex, *P. cinerea* and *P. yagii* all possess a very characteristic cap-like, helmet-like, or hemispherical–cupola-like large aerotope towards the apical cell tip (Böcher, 1949; Niiyama *et al.*, 2016; Tuji & Niiyama, 2016, 2018), these species appear to be cryptic and their differential diagnosis is currently problematic. Therefore, the clearly observable marker of 'galeate' aerotopes can no longer be considered an apomorphic trait of *P. galeata*. The 16S rRNA analyses also showed that the clades of *Pseudanabaena* species with the ability to produce polar aerotopes and special apical cells with large 'galeate' aerotopes are phylogenetically separated and distant, suggesting that these two characters (and the overall presence of aerotopes) are symplesiomorphic for *Pseudanabaena* and shared by several different lineages which diversified independently.

P. pruinosa most closely resembles *P. biceps* (due to its deep constrictions, presence of oval cells, larger aerotopes, and connections of cells mostly at the longitudinal axis; Böcher, 1946, 1949; Figs 1, 4h, 6, 8), then *P. galeata* (due to the hood-like and dome-like apical cell aerotopes, Böcher, 1949) (Fig. 4a–g) and *P. yagii* (due to the occasional presence of sheaths (Tuji & Niiyama, 2018) (Fig. 1b). *P. pruinosa* can be distinguished from these species by the presence of long trichomes with more than 20 cells, closely entangled in parallel or erect fascicles (*P. galeata, P. yagii* and *P. biceps* have shorter few-celled trichomes that lack any additional regular arrangement in erected fascicles or coiled screw-like helices). *P. pruinosa* has also distinctively deeper constrictions than *P. galeata* and *P. yagii*, resulting in cells that are evidently spherical or barrel-shaped (whereas in *P. galeata* and *P. yagii* cells are cylindrical with rounded ends and with less conspicuous constrictions, i.e. 'domino-shaped'); moreover, 'hyaline bridges' are thinner and less evident in *P. pruinosa. P. pruinosa* can be distinguished from *P. biceps* which has acuminate apical cells (Böcher, 1946). The *P. foetida* complex and *P. cinerea* are typically planktic and always have solitary trichomes, not entangled in fascicles and not forming mats (Niiyama *et al.*, 2016; Tuji & Niiyama, 2016, 2018).

As mentioned, the characteristic moniliform trichome appearance of *P. pruinosa*, characterized by the presence of spherical cells, marked constrictions, occasional swollen cells and occasional irregular cell division, are traits shared with *A. gygaxiana*, which lacks aerotopes and sometimes forms enormously long cells (Casamatta *et al.*, 2005; Fig. 4a, 4b). *A. gygaxiana* has similar ecology to *P. pruinosa* (isolated from sub-arctic regions in Canada), and, in this study, we show that phylogenetically it belongs to the *Pseudanabaena sensu stricto* cluster. Moreover, the analysed 1046 bp 16S rRNA fragment (Table 4) of

A. gygaxiana UTCC 393 showed 97.8% identity with *P. pruinosa* NMCCC 001 and 98.0% identity with *P. pruinosa* ULC067 MH118734. *A. gygaxiana* UTCC 393 had the highest 16S rRNA sequence identity with *P. catenata* SAG 1464–1 KM020005 (98.6%). Previous molecular phylogenetic studies have also affiliated *A. gygaxiana* with the Pseudanabaenaceae (Nishizawa *et al.*, 2010; Schirrmeister *et al.*, 2011), while the holotype of the genus, *A. africanum* (Schwabe & Simonsen) Komárek & Lukavsky, belongs to a different and separate clade (Aleksovski, 2015) within the family Leptolyngbyaceae (Strunecký *et al.*, 2023). Casamatta *et al.* (2005) showed that *A. gygaxiana* resolved with *Limnothrix* and *Pseudanabaena* at the base of their phylogenetic tree and that its thylakoid morphology was consistent with that of the Pseudanabaenaceae; nevertheless, they concluded that this taxon belonged in *Arthronema* based on its morphology (i.e. the phenotypic traits of asymmetrical cell division and involution cells, which up to now were considered apomorphic for the genus *Arthronema*). Our study has conclusively shown that this phenotypic trait can also be observed in *Pseudanabaena*. Thus, based on all of the above-mentioned facts, transfer to the genus *Pseudanabaena* is necessary, as proposed below.

Lastly, although bootstrap support is low, it should be noted that this is the first study that shows the position of the genus *Pseudanabaena* sensu stricto within the phylum Cyanobacteria, based on 16S rRNA data. The position of *Pseudanabaena* was previously shown using phylogenomics data (Strunecký *et al.*, 2023), but it was not clear if a tree based only on a single gene (16S RNA gene) would replicate the findings. Our results were congruent with the phylogenomic tree and the phylogenomics data (Strunecký *et al.*, 2023); therefore, we believe that the 16S rRNA phylogenetic analyses in this paper can serve as an initial backbone for gathering further insights into the complex evolution of the Pseudanabaenales.

Pseudanabaena pruinosa *Aleksovski, Krstić, Komárek & Strunecký, sp. nov.*

Description

Thallus forming gelatinous, macroscopic, ovoid balls, 2–8 mm in diameter, or sometimes forming thick gelatinous and structured mats, yellow-green, light green, vivid green, dark green, or olive-green to brownish in colour. Balls and gelatinous mats composed of confluent, amorphous, homogeneous and diffluent masses of mucilage with embedded filaments inside. Single mucilage mass also structured, usually enveloping distinctly divaricated, and richly pseudobranched filaments with evident and characteristic tree-like filament spreading, creating heteropolar gelatinous thallus units with base and wide apical part. Filaments 2.1–8.6 μm wide, with facultative, fine, colourless, clearly widened and evidently branched anastomotic sheaths, with distinctly observable refractive margins. Wide filaments often heteropolar, curved and flexible, containing several to many basal closely entangled, and fasciculated trichomes, and few or solitary trichomes in apical part of single sheath. Trichomes homocytic, uniseriate, isopolar, rarely solitary, mostly closely bundled in clear fascicles of regularly grouped trichomes (2–10), usually in parallel 'erected' positions. Trichomes also often coiled, screw-like, usually forming very characteristic regular voluminous left-handed open helixes embedded in mucilage.

Individual trichomes usually long and typically multi-celled (more than 20 cells), thin, (0.7) 1.2–2.4 (3.0) μm wide, very slightly motile, with intensive and deep constrictions at cross-walls, and distinct moniliform string-of beads outline. Rarely, trichomes show coiled transitions in cell morphology (cells with different shapes within the same trichome and within the same culture), with less intensive constrictions and only with moniliform part of trichome. 'Hyaline bridges' quite thin, with connections between adjacent cells observable mainly around trichome longitudinal axis, close to polar aerotopes, resulting in optical illusion under LM of cells connected or 'glued' by neighbour polar aerotopes.

Cells pale green to vivid green, blue-green, sometimes olive green or brownish to violet, short, 1.2–3.5 (8.2) μm long, usually isodiametric or 1.5× longer than wide, with spherical to distinct barrel-shaped morphology, rarely quadratic with rounded ends. Irregular cell division and presence of elongated cells (up to 8.2 μm long) and swollen cells (up to 3.4 μm wide) observed sometimes. Cell content clearly differentiated in chromatoplasma and centroplasma, with evident parietal arrangement of thylakoids. Cells with both polar, usually large and clearly visible rounded aerotopes (one rounded aerotope per each cell pole) and frequently present central aerotopes, sometimes aerotopes located irregularly throughout whole cells. Cells usually without prominent granules visible by LM, sometimes with rare small facultative indistinct granules. Apical cell spherical to slightly oval, sometimes slightly conical or elongated, with one usually large 'galeate' aerotope at cell tip, forming hood or dome. Reproduction by formation of few-celled hormogonia. Necridic cells absent.

HOLOTYPE HERE DESIGNATED: AS0001MKNH, deposited in the Macedonian National Herbarium at Faculty of Natural Sciences and Mathematics-Skopje (Herbarium Code MKNH), Skopje, North Macedonia.

ISOTYPE HERE DESIGNATED: PMM-B-B-27734, deposited in the National Institution Natural History Museum of North Macedonia – Skopje (Herbarium code: HMMNH), Skopje, North Macedonia.
TYPE STRAIN: *Pseudanabaena pruinosa* NMCCC 001, deposited in the North Macedonian Culture Collection of Cyanobacteria, Skopje, North Macedonia.
ICONOTYPE: Fig. 13.
HABITAT: Isolated from an icy soil crust in the foreland of the valley-type glacier Hørbyebreen, Svalbard. Typical habitats of *P. pruinosa* include hydro-terrestrial ecosystems, as marginal zones and ice forelands of glaciers, fast streams formed from melting glaciers, snow-broth lakes, subnival alpine soil crusts of cyanobacteria growing underneath snow, as well as terrestrial systems (icy microbial soil crusts, cryptobiotic soil crusts). Records include Polar Regions, such as Spitsbergen Island in Svalbard (including Petuniabukta Bay, Ny-Ålesund) and Bylot Island from the Arctic; records from near-polar (sub-Arctic) regions are also known, such as from the Lake Lac-à-l'Eau-Claire in Québec (Canada). Other records include mountains with alpine climates, such as the high Himalayas in Nepal, and the Tien Shan Mountains in China.
TYPE LOCALITY: Arctic, Svalbard Archipelago, central part of the Spitsbergen Island, Billefjorden, northwest of Petuniabukta Bay, foreland of the valley-type glacier Hørbyebreen, icy soil crust (78°55'51"N, 16°37'31"E).
ETYMOLOGY: *pruinosa* (fem. adj.) = frosty.
DIAGNOSTIC CHARACTERS: Presence of both polar and central aerotopes, and rarely, irregular aerotopes located throughout the whole cell, along with the presence of facultative, widened, branched sheaths forming pseudobranched anastomotic filaments with tree-like spread as main apomorphic traits. Other diagnostic characters include: presence of heteropolar, curved and flexible filaments; ability to produce swollen cells and to undergo irregular cell division resulting in some elongated cells; pseudobranched filaments embedded in thick masses of voluminous amorphous mucilage entangling several multi-celled trichomes in fascicles; presence of screw-like left-handed helixes or regularly organized erected fascicles; thin 'hyaline bridges', with connections observable under LM of cells 'glued' together in the central part by their adjacent large polar aerotopes; formation of oval voluminous balls. The new species is distinct also based on the 16S rRNA data.

Pseudanabaena gygaxiana *(Casamatta & Johansen) Aleksovski, Krstić & Strunecký comb. nov.*

BASIONYM: *Arthronema gygaxiana* Casamatta & Johansen in Casamatta *et al.* (2005). *Journal of Phycology* **41**: 429, Fig. 4a,4b.
HOLOTYPE: BRY C-37695.
TYPE LOCALITY: Ontario, Canada. Tasso Lake, Lake of Bays Township, Ontario, Canada.
DISTRIBUTION: Epiphytic in lakes in sub-Arctic regions. Records from Canada, but probably more broadly distributed in ecologically corresponded habitats with freezing temperatures.
TAXONOMIC NOTES: The organism *P. gygaxiana* is morphologically and ecologically mostly similar to *Pseudanabaena pruinosa*. Both *P. pruinosa* and *P. gygaxiana* probably independently diversified from *Pseudanabaena*-like common ancestors under the pressure of extreme ecological conditions of freezing temperatures, which can be supported by phylogenetic evidence and by the sharing of similar phenotypic traits.

Acknowledgements

We would like to express our thanks to Dana Švehlová and Jana Šnokhousová for their technical and professional support, to RNDr. Jiří Košnar and Prof. Dr. Sasho Panov for their support in the molecular analyses as well as to Prof. RNDr. Josef Elster who was responsible for the isolation of most of the strains.

Disclosure statement

No potential conflict of interest was reported by the author(s).

Funding

This work was supported by Czech Science Foundation [Project no: 22-06374S].

Supplementary material

The following supplementary material is accessible via the Supplementary Content tab on the article's online page at https://doi.org/10.1080/09670262.2024.2343088

Supplementary fig. S1. Frequent appearance of characteristic regularly coiled voluminous screw-like helixes in *Pseudanabaena pruinosa*. Scale bar = 10 µm.

References

Aleksovski, B. (2015). Characterization and re-evaluation of selected Pseudanabaenaceae and Leptolyngbyaceae strains using polyphasic approach. short-term scientific mission (STSM): CYANOCOST – ES 1105 action: study of the differences in the polyphyletic gene clusters of genera *Leptolyngbya* and *Pseudanabaena*. CYANOCOST – ES 1105 Action Cyanobacterial Blooms and Toxins In Water Resources: Occurrence, Impacts and Management, December.
Anagnostidis, K. (1961). Untersuchungen über die Cyanophyceen einiger Thermen in Griechenland. *Institut Für Systematische Botanik Und Pflanzengeographie Der Universität Thessaloniki*, **7**: 1–322.

Anagnostidis, K. (2001). Nomenclatural changes in cyanoprokaryotic order Oscillatoriales. *Preslia, Praha*, **73**: 359–375.

Anagnostidis, K. & Komárek, J. (1988). Modern approach to the classification system of cyanophytes 3 - Oscillatoriales. *Algological Studies*, **50**: 327–472.

Averina, S.G., Tsvetikova, S.A., Poliakova, E.Y., Velichko, N.V. & Pinevich, A.V. (2020). Antarctic cyanobacteria of the genus *Pseudanabaena* – an example of psychrotolerant microorganisms. *Issues of Modern Algology*, **2**(**23**): 57–62.

Böcher, T.W. (1946). *Pseudanabaena biceps*, a new sapropelic species from bottom mud. *Botaniska Notiser*, **2**: 281–284.

Böcher, T.W. (1949). Studies on the sapropelic flora of the lake Flyndersø with special reference to the Oscillatoriaceae. *Kongelige Danske Videnskabernes Selskab Biologiske Meddelelser*, **21**: 1–46.

Bohunická, M., Johansen, J.R. & Fucíková, K. (2011). *Tapinothrix clintonii* sp. nov. (Pseudanabaenaceae, Cyanobacteria), a new species at the nexus of five genera. *Fottea*, **11**: 127–140.

Casamatta, D.A., Johansen, J.R., Vis, M.L. & Broadwater, S. T. (2005). Molecular and morphological characterization of ten polar and near-polar strains within the Oscillatoriales (Cyanobacteria). *Journal of Phycology*, **41** (**2**): 421–438.

Darriba, D., Taboada, G.L., Doallo, R. & Posada, D. (2012). jModelTest 2: more models, new heuristics and parallel computing. *Nature Methods*, **9**(**8**): 772.

Davydov, D. (2018). Checklist of cyanobacteria from the European polar desert zone. *Botanica*, **24**(**2**): 185–201.

Garcia, N.A., Pipole, F., da Cunha, L.C., Elias, F., Górniak, S.L. & Sant'Anna, C.L. (2017). Loss of toxicity by *Pseudanabaena galeata* in culture. *Hoehnea*, **44**(**2**): 269–276.

Gomont, M. (1892 '1893'). Monographie des Oscillariées (Nostocacées Homocystées). Deuxième partie. - Lyngbyées. *Annales des Sciences Naturelles, Botanique. Série*, **7**(**16**): 91–264.

Guglielmi, G. & Cohen-Bazire, G. (1984). Etude taxonomique d'un genre de cyanobactérie oscillatoriacée: le genre *Pseudanabaena* Lauterborn. I. Etude ultrastructurale. *Protistologica*, **20**: 377–391.

Hall, T.A. (1999). BioEdit: a user-friendly biological sequence alignment editor and analysis program for windows 95/98/NT. *Nucleic Acids Symposium Series*, **41**: 95–98.

Hiraishi, A. & Kaneko, M. (1994). Use of polymerase chain reaction-amplified 16S rRNA gene sequences to identify pink-pigmented bacteria found in a potable water treatment system. *Bulletin of Japanese Society of Microbial Ecology*, **9**: 55–65.

Iteman, I., Rippka, R., Tandeau de Marsac, N. & Herdman, M. (2000). Comparison of conserved structural and regulatory domains within divergent 16S rRNA-23S rRNA spacer sequences of cyanobacteria. *Microbiology*, **146**(**6**): 1275–1286.

Katoh, K., Misawa, K., Kuma, K. & Miyata, T. (2002). MAFFT: a novel method for rapid multiple sequence alignment based on fast Fourier transform. *Nucleic Acids Research*, **30**(**14**): 3059–3066.

Khan, Z., Omar, W.M.W., Merican, F.M.M.S., Azizan, A.A., Foong, C.P., Convey, P. & Alias, S.A. (2017). Identification and phenotypic plasticity of *Pseudanabaena catenata* from the Svalbard archipelago. *Polish Polar Research*, **38**(**4**): 445–458.

Khan, Z., Wan Omar, W., Mohd Sidik Merican, F., Convey, P., Foong, C.P. & Najimudin, N. (2018). Characterisation of *Pseudanabaena amphigranulata* (Synechococcales) isolated from a man-made pond, Malaysia: a polyphasic approach. *Journal of Applied Phycology*, **30**: 3187–3196.

Komárek, J. & Anagnostidis, K. (2005). *Cyanoprokaryota 2. Teil: Oscillatoriales Vol Süsswasserflora Von Mitteleuropa*. 19/2 ed. Elsevier/Spektrum, Heidelberg.

Komárek, J., Kaštovský, J., Mareš, J. & Johansen, J.R. (2014). Taxonomic classification of Cyanoprokaryotes (Cyanobacterial genera) 2014, using a polyphasic approach. *Preslia*, **86**: 295–335.

Komárek, J., Kovacik, L., Elster, J. & Komárek, O. (2012). Cyanobacterial diversity of Petuniabukta, Billefjorden, central Spitsbergen. *Polish Polar Research*, **33**(**4**): 347–368.

Komárek, J. & Lukavský, J. (1988). *Arthronema*, a new Cyanophyte genus from Afro-Asian deserts. *Algological Studies*, **50-53**: 249–267.

Lauterborn, R. (1915). Die sapropelische Lebewelt. Ein Beitrag zur Biologie des Faulschlammes natürlicher Gewässer. *Verhandlungen Des Naturhistorisch-Medizinischen Vereins Zu Heidelberg*, **2**(**13**): 395–481, pl. III.

Lepère, C., Wilmotte, A. & Meyer, B. (2000). Molecular diversity of *Microcystis* strains (Cyanophyceae, Chroococcales) based on 16S rDNA sequences. *Systematics and Geography of Plants*, **70**(**2**): 275–283.

Lumian, J., Sumner, D., Grettenberger, C., Jungblut, A.D., Pierce-Ward, N.T. & Brown, C.T. (2024). Biogeographic distribution of five antarctic cyanobacteria using large-scale k-mer searching with sourmash branchwater. *Frontiers in Microbiology*, **15**: 1328083.

Mareš, J., Hrouzek, P., Kaňa, R., Ventura, S., Strunecký, O. & Komárek, J. (2013). The primitive thylakoid-less cyanobacterium *Gloeobacter* is a common rock-dwelling organism. *PLOS ONE*, **8**(**6**): e66323.

Mareš, J., Strunecký, O., Bučinská, L. & Wiedermannová, J. (2019). Evolutionary patterns of thylakoid architecture in Cyanobacteria. *Frontiers in Microbiology*, **10**: 277.

Matula, J., Pietryka, M., Richter, D. & Wojtun, B. (2007). Cyanoprokaryota and algae of arctic terrestrial ecosystems in the Hornsund area, Spitsbergen. *Polish Polar Research*, **28**(**4**): 283–315.

Meffert, M.-E. (1987). Planktic unsheathed filaments (Cyanophyceae) with polar and central gas-vacuoles. I: their morphology and taxonomy. *Archiv Für Hydrobiologie – Supplementbände*, **76**: 315–346.

Meffert, M.-E. (1988). *Limnothrix* Meffert nov. gen. - the unsheathed planktic cyanophycean filaments with polar and central gas vacuoles. *Algological Studies*, **50–53**: 269–276.

Morita, R.Y. (1975). Psychrophilic bacteria. *Bacteriological Reviews*, **39**(**2**): 144–167.

Niiyama, Y., Tuji, A., Takemoto, K. & Ichise, S. (2016). *Pseudanabaena foetida* sp. nov. and *P. subfoetida* sp. nov. (Cyanophyta/Cyanobacteria) producing 2–methylisoborneol from Japan. *Fottea*, **16**: 1–11.

Nishizawa, T., Hanami, T., Hirano, E., Miura, T., Watanabe, Y., Takanezawa, A., Komatsuzaki, M., Ohta, H., Shirai, M. & Asayama, M. (2010). Isolation and molecular characterization of a multicellular Cyanobacterium, *Limnothrix*/*Pseudanabaena* sp. strain ABRG5-3. *Bioscience Biotechnology and Biochemistry*, **74**(**9**): 1827–1835.

Nübel, U., Garcia-Pichel, F. & Muyzer, G. (1997). PCR primers to amplify 16S rRNA genes from cyanobacteria. *Applied and Environmental Microbiology*, **63**: 3327–3332.

Pessi, I.S., Pushkareva, E., Lara, Y., Borderie, F., Wilmotte, A. & Elster, J. (2019). Marked succession of cyanobacterial communities following glacier retreat in the high Arctic. *Microbial Ecology*, **77**(**1**): 136–147.

Ronquist, F., Teslenko, M., van der Mark, P., Ayres, D.L., Darling, A., Höhna, S., Larget, B., Liu, L., Suchard, M.A. & Huelsenbeck, J.P. (2012). MrBayes 3.2: efficient Bayesian phylogenetic inference and model choice across a large model space. *Systematic Biology*, **61**(**3**): 539–542.

Schirrmeister, B.E., Antonelli, A. & Bagheri, H.C. (2011). The origin of multicellularity in cyanobacteria. *BMC Evolutionary Biology*, **11**: 45.

Skuja, H. (1948). Taxonomie des Phytoplanktons einiger Seen in Uppland, Sweden. *Symbolae Botanicae Upsalienses*, **9**(**3**): 1–399.

Spurr, A.R. (1969). A low-viscosity epoxy resin embedding medium for electron microscopy. *Journal of Ultrastructure Research*, **26**: 31–43.

Stamatakis, A. (2014). RAxML version 8: a tool for phylogenetic analysis and post-analysis of large phylogenies. *Bioinformatics*, **30**(**9**): 1312–1313.

Strunecký, O., Ivanova, A.P. & Mares, J. (2023). An updated classification of cyanobacterial orders and families based on phylogenomic and polyphasic analysis. *Journal of Phycology*, **59**: 12–51.

Su, H.N., Wang, Q.M., Li, C.Y., Li, K., Luo, W., Chen, B., Zhang, X.Y., Qin, Q.L., Zhou, B.C., Chen, X.L., Zhang, Y.Z. & Xie, B.B. (2017). Structural insights into the cold adaptation of the photosynthetic pigment-protein C-phycocyanin from an Arctic Cyanobacterium. *Biochimica Et Biophysica Acta, Bioenergetics*, **1858**(**4**): 325–335.

Tamura, K., Stecher, G. & Kumar, S. (2021). MEGA 11: molecular evolutionary genetics analysis Version 11. *Molecular Biology and Evolution*, **38**(**7**): 3022–3027.

Tuji, A. & Niiyama, Y. (2016). The identity and phylogeny of *Pseudanabaena* strain, NIES-512, producing 2-methylisoborneol (2-MIB). *Bulletin of the National Museum of Nature and Science, Series B (Botany), Tokyo*, **42**: 83–89.

Tuji, A. & Niiyama, Y. (2018). Two new *Pseudanabaena* (Cyanobacteria, Synechococcales) species from Japan, *Pseudanabaena cinerea* and *Pseudanabaena yagii*, which produce 2-methylisoborneol. *Phycological Research*, **66**: 291–299.

Woo, P.C., Leung, P.K., Leung, K.W. & Yuen, K.Y. (2000). Identification by 16S ribosomal RNA gene sequencing of an Enterobacteriaceae species from a bone marrow transplant recipient. *Molecular Pathology*, **53**(**4**): 211–215.

Zuker, M. (2003). Mfold web server for nucleic acid folding and hybridization prediction. *Nucleic Acids Research*, **31** (**13**): 3406–3415.